

The Superconformal Index of Class \mathcal{S} Theories of Type D

Madalena Lemos^{*}, Wolfger Peelaers[†], Leonardo Rastelli[‡]

*C.N. Yang Institute for Theoretical Physics,
Stony Brook University,
Stony Brook, NY 11794-3840, USA*

ABSTRACT: We consider the superconformal index of class \mathcal{S} theories of type D , which arise by compactification of the $(2,0)$ D_n theories on a punctured Riemann surface \mathcal{C} . We also allow for the presence of twist lines on \mathcal{C} associated to the \mathbb{Z}_2 outer automorphism of D_n . For the two-parameter slice $(p=0, q, t)$ in the space of superconformal fugacities, we determine the $2d$ TQFT that computes the index.

^{*}madalena.lemos@stonybrook.edu

[†]wolfer.peelaers@stonybrook.edu

[‡]leonardo.rastelli@stonybrook.edu

Contents

1. Introduction	1
2. Class \mathcal{S} Theories of Type D	3
3. A TQFT with Twist Lines	7
3.1 Preliminaries	8
3.2 TQFT structure	9
3.3 D_2 theories	12
3.3.1 Hall-Littlewood limit	12
3.3.2 Schur limit	14
3.3.3 Macdonald limit	14
3.3.4 D_2 theories in terms of A_1 theories	15
3.4 D_3 theories	16
3.5 D_n theories	17
4. Partially Closed Punctures	18
4.1 Classification	18
4.2 The index with partially closed punctures	20
4.2.1 Fugacities corresponding to Young diagram	20
4.2.2 \mathcal{K} -factors	22
A. Macdonald Polynomials and Macdonald Operator	25
A.1 Weyl invariant polynomials and the Macdonald operator	25
A.2 More explicit expressions for the C - and D -series	28
A.2.1 The case $C_n = \mathrm{USp}(2n)$	28
A.2.2 The case $D_n = \mathrm{SO}(2n)$	29
B. Interwining Property of the Free Hyper Index	29

1. Introduction

Class \mathcal{S} theories are a family of four-dimensional gauge theories with $\mathcal{N} = 2$ supersymmetry, which arise by (partially twisted) compactification of the six-dimensional $(2, 0)$ theories on a punctured Riemann surface [1, 2]. There is a beautiful dictionary relating supersymmetric observables of the $4d$ theory with quantities defined on the surface \mathcal{C} . Notably, the complex structure moduli of \mathcal{C} correspond to the exactly marginal $4d$ gauge couplings, while the punctures are associated to flavor symmetries. The partition function of the $4d$ theory on

S^4 is computed by a conformal field theory correlator on \mathcal{C} [3]. Here we focus on the item of the $4d/2d$ dictionary introduced in [4]: the $S^3 \times S^1$ partition function of a superconformal theory of class \mathcal{S} , also known as the superconformal index [5, 6] (henceforth simply the index), is computed by a topological QFT (TQFT) correlator on \mathcal{C} .

The $(2, 0)$ theories are isolated superconformal field theories labeled by the simply laced Lie algebras, $\{A_n, D_n, E_6, E_7, E_8\}$. Correspondingly, there are class \mathcal{S} theories of type A , D and E . To characterize the $4d$ theory one needs to further specify the punctured surface \mathcal{C} , together with some extra discrete data associated to each puncture, which determine the flavor group associated to the puncture [1, 7, 8, 9, 10, 11]. This construction can be further enriched [7, 8] by decorating \mathcal{C} with topologically non-trivial “twist lines” (ending at a puncture or wrapping a cycle), associated to the outer automorphism group of the simply laced Lie algebra (which is \mathbb{Z}_2 in all cases except D_4 , when it is \mathbb{Z}_3).

For all theories of type A , and in the absence of twist lines, the superconformal index has been completely determined in a series of papers [4, 12, 13, 14, 15]¹, by characterizing the associated $2d$ TQFT. The TQFT is defined abstractly in terms of its structure constants $C_{\alpha\beta\gamma}$ (corresponding to three-punctured spheres) and propagators $\eta^{\alpha\beta}$ (corresponding to two-punctured spheres), where α, β, γ label A_n irreducible representations. For a two-dimensional slice $(p = 0, q, t)$ in fugacity space, the answer takes an elegant closed form involving Macdonald polynomials, and the TQFT is recognized as q -deformed $2d$ Yang-Mills [18] in the zero area limit² for $q = t$, and as a certain refinement thereof for $q \neq t$ [21, 22]. This result was originally found in [13, 14] by focussing on the A_1 theories, which have a Lagrangian description, and finding a basis of functions where the structure constants are diagonal (*i.e.*, $C_{\alpha\beta\gamma} = 0$ unless $\alpha = \beta = \gamma$). Since these functions are closely related to Macdonald polynomials, which are defined for any root system, a general answer can be naturally conjectured for all A_n theories [14].

The conjecture of [14] was recently proved in [15], and in fact extended to arbitrary (p, q, t) , under the sole assumption that class \mathcal{S} theories enjoy generalized S-duality, which is the statement that different pairs-of-pants decomposition of \mathcal{C} correspond to the same $4d$ theory in different duality frames. Schematically, the strategy of [15] was to derive certain difference equations for the index, by considering its singularity structure (the residues at the flavor fugacities poles) in distinct, but by assumption equivalent, duality frames. These difference equations have unique solutions and thus completely characterize the index. In particular, the eigenfunctions $\{\psi_\alpha(\mathbf{a})\}$ of the difference operators define the basis where the structure constants $C_{\alpha\beta\gamma}$ are diagonal. For arbitrary (p, q, t) , the difference operators are closely related to the elliptic RS operators, whose eigenfunctions are not known in closed form, but for $p = 0$ they are related to the well-known Macdonald operators, whose eigenfunctions are the Macdonald polynomials. Acting with a difference operator on the index has the physical interpretation [15] of decorating the $4d$ theory by the insertion of a BPS surface defect.

In this paper we enlarge the setup to include class \mathcal{S} theories of type D , also allowing for

¹See also [16, 17] for the evaluation of the index in the presence of BPS line defects and domain walls.

²See [19, 20] for a recent top-down argument that recovers $2d$ q YM by localization of $5d$ super Yang-Mills on S^3 .

the possibility of \mathbb{Z}_2 twist lines on \mathcal{C} . In type D theories, twist lines are very natural, indeed they are necessary for the description of all the non-trivial examples with a Lagrangian, such as the superconformal linear quivers with alternating SO/USp gauge groups [7, 8]. Ideally, one would generalize the approach of [15], and derive the general answer with no guesswork. However this seems technically challenging, because conformal tails of type D have no analog of the $U(1)$ flavor punctures that were used in [15] to derive the difference operators. Thinking about the physics of surface operators may provide the right clues, but we leave this for the future. Here we generalize instead the approach of [14], and look for a diagonal representation of the index for $p = 0$ in the Macdonald basis. The presence of twist lines makes the story richer, leading to an interesting extension of $2d$ TQFT structure. As in [15], we get some mileage by considering the action of Macdonald difference operators. In particular we use these difference operators to argue that the index of free hypermultiplets has a diagonal expansion in the Macdonald basis. In this paper the difference operators serve an auxiliary technical role, but it is natural to expect that they also have a physical interpretation in terms of BPS surface defects.

The rest of the paper is organized as follow. In section 2 we review some facts about the class \mathcal{S} theories of type D , with or without \mathbb{Z}_2 twist lines. In section 3, after briefly recalling the definition of the superconformal index and the TQFT approach, we consider the special cases of D_2 and D_3 theories, and extrapolate from them our general proposal for the D_n case (with maximal and empty punctures). In section 4 we consider the extension to partially closed punctures. In appendix A we collect some technical background material on Macdonald theory. Finally appendix B contains the main intertwining identity that shows diagonality of the free hyper index in the Macdonald basis.

Note added: Last night, the interesting article [23] appeared on the ArXiv. The authors of [23] focus on the evaluation of the index twisted³ by the outer automorphism group along the temporal S^1 , while we focus instead on the ordinary (untwisted) index of type D theories but with twist lines on \mathcal{C} , so our results are largely complementary to theirs. There is some partial overlap in the discussion of the purely SO theories.

2. Class \mathcal{S} Theories of Type D

The superconformal theories that we consider were constructed in [7, 8] following [1]. Let us briefly summarize the relevant points.

First recall that an $\mathcal{N} = 2$ hypermultiplet in representation R of the gauge group G can be decomposed in two $\mathcal{N} = 1$ chiral multiplets sitting in complex conjugate representations R and R^* . The flavor symmetry of N_f such hypermultiplets depends on the reality properties of the representation R . For R complex one has flavor symmetry $U(N_f)$; for R real, the flavor symmetry is enhanced to $\text{USp}(2N_f)$; for R pseudoreal the flavor symmetry is enlarged to $\text{SO}(2N_f)$. For pseudoreal R , there is no need to double the multiplet to satisfy CPT, and one can consider a single chiral multiplet in representation R as an $\mathcal{N} = 2$ multiplet. This is the so-called half-hypermultiplet. However, to avoid Witten’s global anomaly

³For the case of $\mathcal{N} = 4$ SYM, such twisted index was also studied in [24]. The compactification of the $(2, 0)$ theory on a circle with automorphism twist was studied in [25].

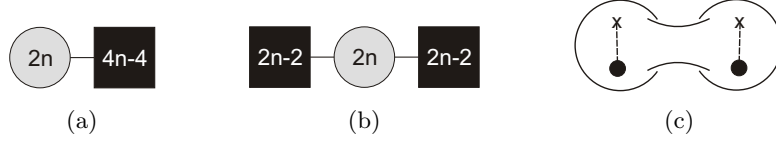


Figure 1: Quiver and corresponding curve for the $\text{SO}(2n)$ gauge theory with $N_f = 2n - 2$ hypermultiplets in the vector representation of $\text{SO}(2n)$.

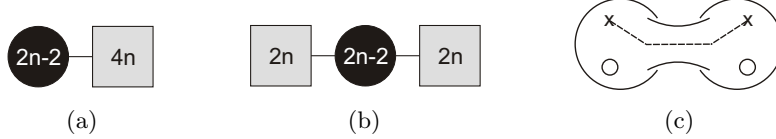


Figure 2: Quiver and corresponding curve for the $\text{USp}(2n - 2)$ gauge theory with $N_f = 2n$ hypermultiplets in the fundamental representation of $\text{USp}(2n - 2)$.

[26] one cannot have an odd number of half-hypermultiplets. N_f half-hypermultiplets have $\text{SO}(N_f)$ flavor symmetry.

In order to construct superconformal theories, all couplings need to be marginal. For gauge group $\text{SO}(m)$ with hypermultiplets in the vector representation this implies that $N_f = m - 2$, and then the flavor symmetry is $\text{USp}(2m - 4)$. For gauge group $\text{USp}(2n)$ with hypermultiplets in the fundamental representation the requirement is that $N_f = 2n + 2$, and the flavor symmetry is given by $\text{SO}(4n + 4)$. It is possible to consider half-hypermultiplets in this case.

Given these constraints, one can start constructing superconformal quiver gauge theories. In order to be superconformal, these will in general have alternating gauge groups. Let us briefly introduce our quiver conventions which follow [7]. A gauge group is depicted by a circle, grey when SO and black for USp . Numbers inside the circles indicate which SO or USp gauge group is considered. Lines connecting two gauge groups represent bifundamental⁴ half-hypermultiplets. Additional hypermultiplets are denoted by squares. Grey squares indicate that they carry SO flavor symmetry, and black ones USp flavor symmetry. Numbers inside the boxes indicate which flavor symmetry they have. The simplest example is to consider an $\text{SO}(2n)$ gauge theory coupled to $N_f = 2n - 2$ hypermultiplets. The flavor symmetry is $\text{USp}(4n - 4)$. This theory is depicted in figure 1a. In figure 1b one focuses on a $\text{USp}(2n - 2) \times \text{USp}(2n - 2)$ subgroup of this flavor symmetry group. This quiver theory can also be depicted in terms of the curve \mathcal{C} in figure 1c. Here the SO gauge group is depicted by a cylinder and each three-punctured sphere represents a free half-hypermultiplet transforming under the fundamental of $\text{USp}(2n - 2)$, corresponding to the puncture denoted by the symbol \bullet , and the vector of $\text{SO}(2n)$, depicted by the symbol \circ . In this case the diagonal SO group is gauged. Also notice the presence of a \mathbb{Z}_2 twist line connecting the USp puncture and the empty USp flavor symmetry puncture (drawn as \times), in the curve. Similarly one can consider a $\text{USp}(2n - 2)$ gauge theory coupled to $N_f = 2n$

⁴More precisely, the word “fundamental” means the vector representation of SO and the fundamental representation of USp

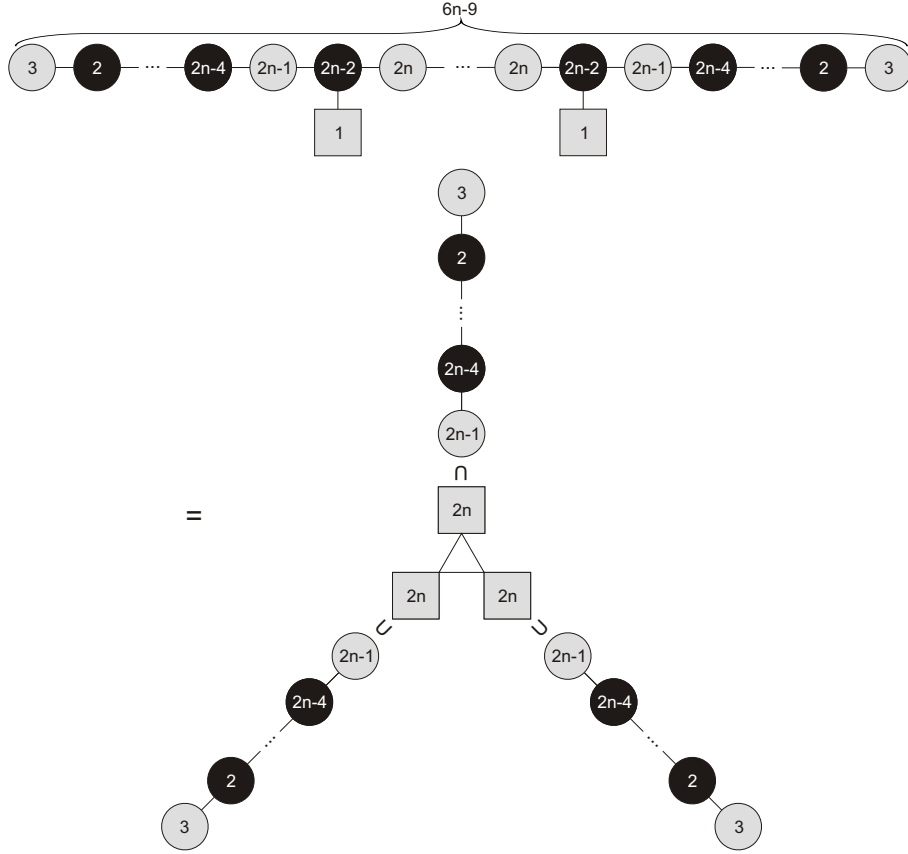


Figure 3: Construction of the $T_{\text{SO}(2n)}$ theory. The \dots in the middle of the top quiver stand for a sequence of alternating $\text{SO}(2n)$ and $\text{USp}(2n-2)$ gauge groups. The other \dots on the left/right stand for a sequence of alternating odd SO and USp gauge groups of increasing/decreasing rank. The symbol \subset means that we gauge a $\text{SO}(2n-1)$ subgroup of $\text{SO}(2n)$.

hypermultiplets. Figure 2 depicts this theory. Here the USp gauge group is denoted by a cylinder with a twist line.

Starting with linear quivers, which have a Lagrangian description, one can make use of dualities to obtain new interacting theories. Figure 3 summarizes the construction of the so-called $T_{\text{SO}(2n)}$ theory [7]. It is described by a three-punctured sphere with three $\text{SO}(2n)$ punctures. The effective number of hyper- and vectormultiplets for this theory is [7]

$$n_V = \frac{8n^3}{3} - 7n^2 + \frac{10n}{3}, \quad n_H = \frac{8n^3}{3} - 4n^2 + \frac{4n}{3}. \quad (2.1)$$

Notice that for $n = 2$ one finds that the effective number of vectormultiplets is zero. Figure 4 summarizes the construction of another interacting theory [27], denoted as $\tilde{T}_{\text{SO}(2n)}$, which is described by a sphere with two $\text{USp}(2n-2)$ punctures and one $\text{SO}(2n)$ puncture. The effective number of hyper- and vectormultiplets for this theory is [27]

$$n_V = \frac{8n^3}{3} - 7n^2 + \frac{16n}{3} - 1, \quad n_H = \frac{8n^3}{3} - 4n^2 + \frac{4n}{3}. \quad (2.2)$$

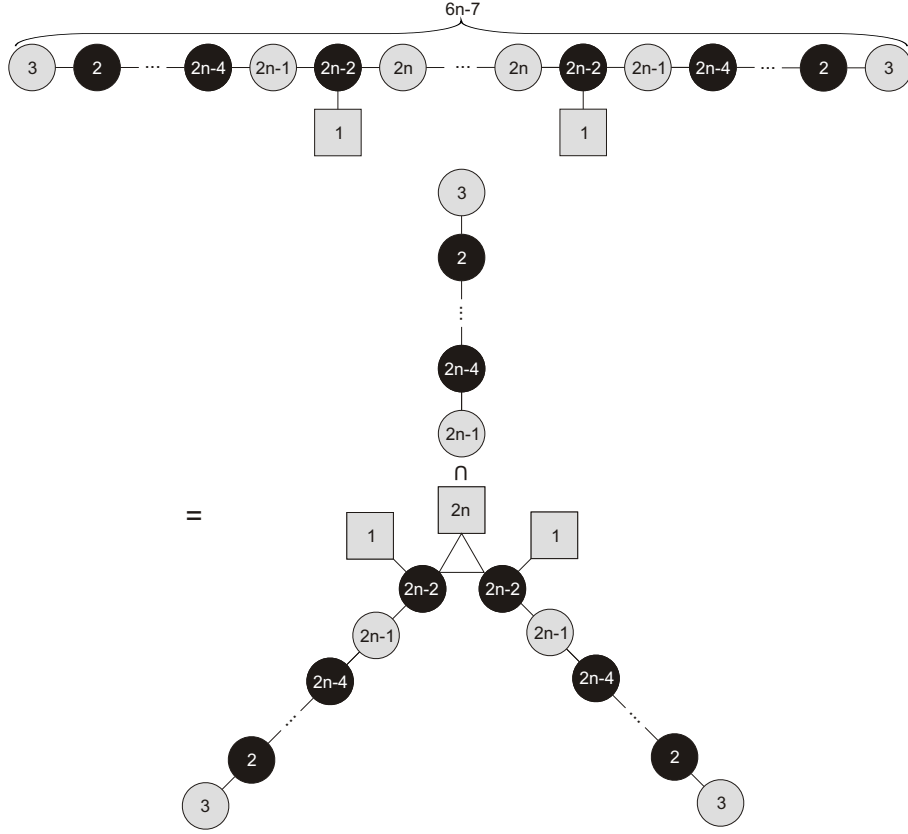


Figure 4: Construction of the $\tilde{T}_{SO(2n)}$ theory. The \dots in the middle of the top quiver stand for a sequence of alternating $SO(2n)$ and $USp(2n-2)$ gauge groups. The other \dots on the left/right stand for a sequence of alternating odd SO and USp gauge groups of increasing/decreasing rank. The symbol \subset means that we gauge a $SO(2n-1)$ subgroup of $SO(2n)$.

Finally, there is one more basic three-punctured sphere we can introduce and that will only appear as part of a bigger theory, namely a sphere with an $SO(2n)$ puncture and two empty USp punctures \times .

Gluing two punctures by a cylinder corresponds as always to gauging the diagonal flavor group. By gluing the basic three-punctured spheres introduced so far, see figure 5, we can generate punctured surfaces of arbitrary topology, subject to the condition that the USp punctures must come in an even number, and be connected pairwise by twist lines. There can also be twist lines wrapping the a -cycles of the surface. Different duality frames correspond to different degeneration limits of the same surface [1]. Basic examples are given in figure 6.

The class of surfaces generated by the three-punctured spheres figure 5 correspond to the smallest subclass of theories that contains the alternating linear quivers with $SO(2n)$ and $USp(2n-2)$ gauge groups and is closed under S-dualities. More general superconformal tails will be incorporated in section 4 by considering more general punctures.

$$\begin{aligned}
\mathcal{I}(\mathbf{a}, \mathbf{b}) &= \text{(a)} \quad \text{Diagram: A circle with a small white circle labeled 'a' at the top and a small black circle labeled 'b' at the bottom. A dashed line with 'x' at both ends connects them.} \\
\mathcal{I}_{T_{\text{SO}(2n)}}(\mathbf{a}_1, \mathbf{a}_2, \mathbf{a}_3) &= \text{(b)} \quad \text{Diagram: A circle with three small white circles labeled 'a_1', 'a_2', and 'a_3' inside.} \\
\mathcal{I}(\mathbf{a}) &= \text{(c)} \quad \text{Diagram: A circle with a small white circle labeled 'a' at the top and two 'x' marks at the bottom. A dashed line connects the two 'x' marks.} \\
\mathcal{I}_{\tilde{T}_{\text{SO}(2n)}}(\mathbf{a}, \mathbf{b}_1, \mathbf{b}_2) &= \text{(d)} \quad \text{Diagram: A circle with a small white circle labeled 'a' at the top, and two small black circles labeled 'b_1' and 'b_2' at the bottom. A dashed line connects them.}
\end{aligned}$$

Figure 5: The three-punctured spheres with maximal SO punctures and maximal or empty USp punctures. We indicate the flavor fugacity assignments and our notation for the corresponding index.

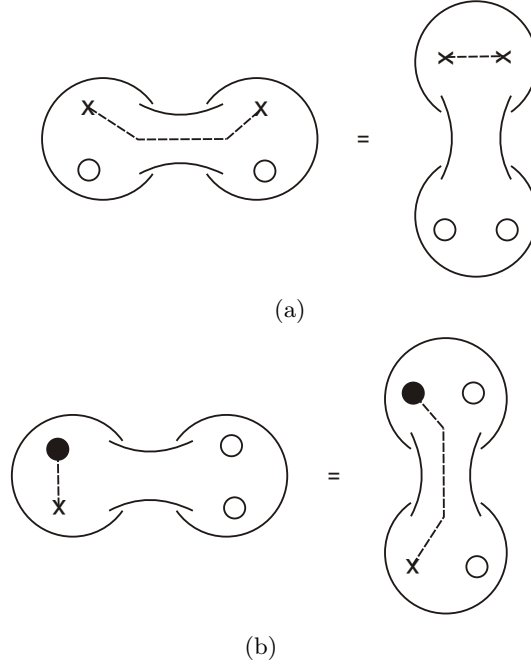


Figure 6: Two examples of S-duality.

3. A TQFT with Twist Lines

In this section we determine the $2d$ TQFT that computes the $p = 0$ limit of the index for the theories described in the previous section. Our starting point is the plausible guess that the Macdonald basis should diagonalize the structure constants of the TQFT. The presence of twist lines and of punctures of both SO and USp type leads however to a more involved structure. Indeed we will have to deal with these complications already in the basic example of free hypers. Nevertheless, we are led to a natural proposal that passes several checks.

3.1 Preliminaries

Let us recap some basic fact about the $\mathcal{N} = 2$ superconformal index. We follow the notations and conventions of [14]. The index [5] is defined by a trace over the states on S^3 (in the standard radial quantization of the CFT),

$$\mathcal{I}(p, q, t) = \text{Tr} (-1)^F \left(\frac{t}{pq} \right)^r \left(\frac{p}{q} \right)^{j_1} (pq)^{j_2} t^R \prod_i a_i^{f_i}. \quad (3.1)$$

Here $j_{1,2}$ are the Cartans of the Lorentz group $SU(2)_1 \times SU(2)_2$, r is the $U(1)_r$ generator, R is the Cartan of $SU(2)_R$ and f_i are flavor symmetry charges. The combinations of superconformal generators in (3.1) commute with the supercharge \tilde{Q}_{1-} which carries quantum numbers $j_1 = 0$, $j_2 = -\frac{1}{2}$, $r = -\frac{1}{2}$ and $R = \frac{1}{2}$ and with its conjugate. The index counts states in the cohomology of \tilde{Q}_{1-} . In particular only states satisfying

$$2 \left\{ \tilde{Q}_{1-}, \left(\tilde{Q}_{1-} \right)^\dagger \right\} = E - 2j_2 - 2R + r = 0 \quad (3.2)$$

contribute. For theories with a Lagrangian description the index can be computed as a matrix integral, which can be written schematically as

$$\mathcal{I}(V, p, q, t) = \int [dU] \exp \left(\sum_{n=1}^{+\infty} \frac{1}{n} \sum_j f^{(j)}(p^n, q^n, t^n) \cdot \chi_{\mathcal{R}_j}(U^n, V^n) \right). \quad (3.3)$$

Here U collectively denotes all gauge group elements and V all flavor group elements, while $[dU]$ denotes the invariant Haar measure for all gauge groups⁵. The sum over j runs over all the $\mathcal{N} = 2$ supermultiplets in the Lagrangian. The symbol \mathcal{R}_j denotes the representation of the j -th supermultiplet under the flavor and gauge groups, and $\chi_{\mathcal{R}_j}$ is its character. Finally $f^{(j)}$ denotes the single-letter indices, which are given

$$f^V = -\frac{p}{1-p} - \frac{q}{1-q} + \frac{pq/t - t}{(1-q)(1-p)}, \quad (3.4)$$

$$f^{\frac{1}{2}H} = \frac{\sqrt{t} - pq/\sqrt{t}}{(1-q)(1-p)}, \quad (3.5)$$

for an $\mathcal{N} = 2$ vectormultiplet and an $\mathcal{N} = 2$ half-hypermultiplet respectively.

Several limits of the index (3.1) with enhanced supersymmetry can be considered. For $p \rightarrow 0$, one obtains what was called the Macdonald index in [14]. This index counts states annihilated by both \tilde{Q}_{1-} and Q_{1+} , and thus is a $\frac{1}{4}$ BPS object. If in addition one takes $q \rightarrow 0$, one obtains the Hall-Littlewood index, which counts states annihilated by \tilde{Q}_{1-} , Q_{1+} and Q_{1-} . Finally, taking $q = t$ and p arbitrary results in the Schur index, which in fact turns out to be independent of p . In this paper we will focus on these limits of enhanced supersymmetry.

⁵In the notation of appendix A, it would be a product over all gauge groups of factors of the form $[da]\Delta(a)$.

3.2 TQFT structure

Following the logic of [4], we wish to identify the TQFT associated to the index of type D theories of class \mathcal{S} , in the enhanced supersymmetry limit $p = 0$ (the “Macdonald index”). In this section we restrict to theories with maximal and empty punctures. The basic building blocks are the three-punctured spheres in figure 5 and the cylinders (propagators).

There are two types of propagators: with or without a twist line running along the cylinder, corresponding respectively to USp and SO gauge groups. They are given by

$$\begin{aligned}\eta_{\mathrm{SO}}(\mathbf{a}_1, \mathbf{a}_2) &= \Delta_{\mathrm{SO}}(\mathbf{a}_1) \mathcal{I}_{\mathrm{SO}}^V(\mathbf{a}_1) \delta(\mathbf{a}_1, \mathbf{a}_2^{-1}), \\ \eta_{\mathrm{USp}}(\mathbf{b}_1, \mathbf{b}_2) &= \Delta_{\mathrm{USp}}(\mathbf{b}_1) \mathcal{I}_{\mathrm{USp}}^V(\mathbf{b}_1) \delta(\mathbf{b}_1, \mathbf{b}_2^{-1}),\end{aligned}\tag{3.6}$$

where $\Delta_{\mathrm{SO}}(\mathbf{a})$ and $\Delta_{\mathrm{USp}}(\mathbf{a})$ denote the $\mathrm{SO}(2n)$ and $\mathrm{USp}(2n-2)$ Haar measures respectively. The index for a general vectormultiplet is known explicitly:

$$\begin{aligned}\mathcal{I}^V &= \mathrm{PE}[f^V \chi^{adj}] \\ &= (q; q)_\infty^r (t; q)_\infty^r \prod_{\alpha \in R} (qe^\alpha; q)_\infty (te^\alpha; q)_\infty.\end{aligned}\tag{3.7}$$

Here the plethystic exponential PE is defined as $\mathrm{PE}[f(x_i)]_{x_i} \equiv \exp(\sum_{n=1}^\infty \frac{1}{n} f(x_i^n))$, and the q -Pochhammer symbol as $(a; q)_\infty = \prod_{j=0}^\infty (1 - aq^j)$. Usually, we omit the subscript in the plethystic exponential and take it with respect to all parameters. Moreover, f^V is the single letter partition function for the vectormultiplet (3.4) in the Macdonald limit ($p \rightarrow 0$), $\chi^{adj} = r + \sum_{\alpha \in R} e^\alpha$ the adjoint character, and r denotes the rank of the group. More concretely, one has for the $\mathrm{SO}(2n)$ and $\mathrm{USp}(2n-2)$ vectormultiplet indices

$$\mathcal{I}_{\mathrm{SO}}^V(\mathbf{a}) = (q, t; q)_\infty^n \prod_{i < j} \left(q a_i^\pm a_j^\pm, t a_i^\pm a_j^\pm; q \right)_\infty, \tag{3.8}$$

$$\mathcal{I}_{\mathrm{USp}}^V(\mathbf{b}) = (q, t; q)_\infty^{n-1} \prod_{\alpha} \left(q b_\alpha^{\pm 2}, t b_\alpha^{\pm 2}; q \right)_\infty \prod_{\alpha < \beta} \left(q b_\alpha^\pm b_\beta^\pm, t b_\alpha^\pm b_\beta^\pm; q \right)_\infty, \tag{3.9}$$

where a_i , $i = 1, \dots, n$, and b_α , $\alpha = 1, \dots, n-1$, denote fugacities of SO and USp respectively. Here and throughout the paper we use the condensed notation that \pm means we take the product over all sign choices and $(x_1, \dots, x_l; q)_\infty = \prod_{k=1}^l (x_k; q)_\infty$.

The indices of the different three-punctured spheres are parametrized as in figure 5. All of these are a priori unknown functions of the flavor symmetry fugacities and q and t , except for the free half-hypermultiplet index $\mathcal{I}(\mathbf{a}, \mathbf{b})$, which reads

$$\begin{aligned}\mathcal{I}(\mathbf{a}, \mathbf{b}) &= \mathrm{PE}[f^{\frac{1}{2}H} \chi_{\mathrm{SO}(2n)}^v(\mathbf{a}) \chi_{\mathrm{USp}(2n-2)}^f(\mathbf{b})] \\ &= \prod_{i=1}^n \prod_{\alpha=1}^{n-1} \frac{1}{(\sqrt{t} a_i^\pm b_\alpha^\pm; q)_\infty}.\end{aligned}\tag{3.10}$$

Here $\chi_{\mathrm{SO}(2n)}^v$ and $\chi_{\mathrm{USp}(2n-2)}^f$ are the characters of the vector representation of $\mathrm{SO}(2n)$ and the fundamental representation of $\mathrm{USp}(2n-2)$, respectively.

Following [14], we expand the free hypermultiplet index in two complete bases of functions $\{f_{\text{SO}}^\lambda(\mathbf{a})\}$ and $\{f_{\text{USp}}^{\lambda'}(\mathbf{b})\}$, labeled by $\text{SO}(2n)$ and $\text{USp}(2n-2)$ representations respectively,

$$\mathcal{I}(\mathbf{a}, \mathbf{b}) = \sum_{\lambda, \lambda'} C_{\lambda, \lambda'} f_{\text{SO}}^\lambda(\mathbf{a}) f_{\text{USp}}^{\lambda'}(\mathbf{b}) . \quad (3.11)$$

These functions are chosen to be orthonormal under the measure which appears in each of the propagators

$$\begin{aligned} \oint [d\mathbf{a}_1] \oint [d\mathbf{a}_2] \eta_{\text{SO}}(\mathbf{a}_1, \mathbf{a}_2) f_{\text{SO}}^{\lambda_1}(\mathbf{a}_1) f_{\text{SO}}^{\lambda_2}(\mathbf{a}_2) &= \delta^{\lambda_1 \lambda_2} , \\ \oint [d\mathbf{b}_1] \oint [d\mathbf{b}_2] \eta_{\text{USp}}(\mathbf{b}_1, \mathbf{b}_2) f_{\text{USp}}^{\lambda'_1}(\mathbf{b}_1) f_{\text{USp}}^{\lambda'_2}(\mathbf{b}_2) &= \delta^{\lambda'_1 \lambda'_2} . \end{aligned} \quad (3.12)$$

We will now show that we can find bases such that the structure constants, $C_{\lambda, \lambda'}$, are “diagonal” in the sense that only some of the $\text{SO}(2n)$ representations appear in the sum, which are in one-to-one correspondence with all representations of $\text{USp}(2n-2)$. As in [14] we consider the following Ansätze

$$f_{\text{SO}}^\lambda(\mathbf{a}) = \mathcal{K}_{\text{SO}}(\mathbf{a}) P_{\text{SO}}^\lambda(\mathbf{a}) , \quad f_{\text{USp}}^{\lambda'}(\mathbf{b}) = \mathcal{K}_{\text{USp}}(\mathbf{b}) P_{\text{USp}}^{\lambda'}(\mathbf{b}) , \quad (3.13)$$

with the factors \mathcal{K} chosen such that the polynomials P^λ are orthonormal under the new measures

$$\hat{\Delta}_{\text{SO}}(\mathbf{a}) \equiv \mathcal{I}_{\text{SO}}^V(\mathbf{a}) \mathcal{K}_{\text{SO}}(\mathbf{a}) \mathcal{K}_{\text{SO}}(\mathbf{a}^{-1}) \Delta_{\text{SO}}(\mathbf{a}) , \quad (3.14)$$

$$\hat{\Delta}_{\text{USp}}(\mathbf{b}) \equiv \mathcal{I}_{\text{USp}}^V(\mathbf{b}) \mathcal{K}_{\text{USp}}(\mathbf{b}) \mathcal{K}_{\text{USp}}(\mathbf{b}^{-1}) \Delta_{\text{USp}}(\mathbf{b}) . \quad (3.15)$$

We shall see that if we take the two complete sets of functions P^λ ⁶ to be the Macdonald polynomials for the SO and USp groups, the structure constants are “diagonal”. This means that $\hat{\Delta}$ will be the Macdonald measure defined in equation (A.4), and this fixes the \mathcal{K} -factors to be

$$\mathcal{K} = \frac{1}{(q; q)_\infty^{r/2} (t; q)_\infty^{r/2}} \prod_{\alpha \in R} \frac{1}{(te^\alpha; q)_\infty} , \quad (3.16)$$

where we made use of (A.5) and (3.7) and the obvious invariance under negating roots.

To show the “diagonality”, we act on the index of the free hyper with both the $\text{SO}(2n)$ and $\text{USp}(2n-2)$ Macdonald operators (equations (A.16) and (A.18)), conjugated by the respective \mathcal{K} -factor, and find that (see appendix B)

$$\mathcal{K}_{\text{SO}}(\mathbf{a}) D_{\text{SO}} \mathcal{K}_{\text{SO}}^{-1}(\mathbf{a}) \mathcal{I}(\mathbf{a}, \mathbf{b}) = \mathcal{K}_{\text{USp}}(\mathbf{b}) D_{\text{USp}} \mathcal{K}_{\text{USp}}^{-1}(\mathbf{b}) \mathcal{I}(\mathbf{a}, \mathbf{b}) . \quad (3.17)$$

Since the Macdonald polynomials are eigenfunctions of D , the functions f^λ will be eigenfunctions of $\mathcal{K} D \mathcal{K}^{-1}$ with non-degenerate eigenvalues c^λ . Using the expansion of the index this means that

$$\sum_{\lambda, \lambda'} c_{\lambda'}^{\text{USp}} C_{\lambda, \lambda'} f_{\text{SO}}^\lambda(\mathbf{a}) f_{\text{USp}}^{\lambda'}(\mathbf{b}) = \sum_{\lambda, \lambda'} c_\lambda^{\text{SO}} C_{\lambda, \lambda'} f_{\text{SO}}^\lambda(\mathbf{a}) f_{\text{USp}}^{\lambda'}(\mathbf{b}) . \quad (3.18)$$

⁶Note that the Macdonald polynomials as defined in equation (A.8) are only orthogonal, and so one needs to normalize them to have unit inner product. P^λ is used to denote the normalized polynomials.

As noted in appendix A.2 we have $c_{(\lambda'_1, \dots, \lambda'_{n-1})}^{\text{USp}} = c_{(\lambda'_1, \dots, \lambda'_{n-1}, \lambda'_{n-1})}^{\text{SO}}$, where λ'_i denotes the Dynkin labels of the representation λ' . This, together with the non-degeneracy of the eigenvalues c_λ^{SO} , implies that the expansion of the index in equation (3.11) is “diagonal” in the sense that for any $\text{USp}(2n-2)$ representation $\lambda' = (\lambda'_1, \dots, \lambda'_{n-1})$

$$C_{\lambda, \lambda'} \neq 0 \quad \Rightarrow \quad \lambda = (\lambda'_1, \dots, \lambda'_{n-1}, \lambda'_{n-1}) , \quad (3.19)$$

hence the sum runs over all $\text{USp}(2n-2)$ representations.

The index of $T_{\text{SO}(2n)}$ can also be expanded in the set of functions $\{f_{\text{SO}}^\lambda(\mathbf{a})\}$

$$\mathcal{I}_{T_{\text{SO}(2n)}}(\mathbf{a}_1, \mathbf{a}_2, \mathbf{a}_3) = \sum_{\lambda_1, \lambda_2, \lambda_3} B_{\lambda_1, \lambda_2, \lambda_3} f_{\text{SO}}^{\lambda_1}(\mathbf{a}_1) f_{\text{SO}}^{\lambda_2}(\mathbf{a}_2) f_{\text{SO}}^{\lambda_3}(\mathbf{a}_3) . \quad (3.20)$$

Motivated by the structure of the T_N theory index of [14, 15] we assume that the basis of functions which diagonalizes the $C_{\lambda, \lambda'}$ also diagonalizes the B structure constants,⁷

$$B_{\lambda_1, \lambda_2, \lambda_3} \neq 0 \Rightarrow \lambda_1 = \lambda_2 = \lambda_3 . \quad (3.21)$$

Note that the sum in (3.20) runs over all $\text{SO}(2n)$ representations.

The S-dualities shown in figure 6 can be written in simple form if we also expand the indices of the three-punctured spheres in figures 5c and 5d in the $\{f_{\text{SO}}^\lambda(\mathbf{a})\}$ and $\{f_{\text{USp}}^{\lambda'}(\mathbf{b})\}$ bases, and can be used to constrain the structure constants of these spheres. We write the indices of these spheres as

$$\mathcal{I}_{\tilde{T}_{\text{SO}(2n)}}(\mathbf{a}, \mathbf{b}_1, \mathbf{b}_2) = \sum_{\lambda, \lambda'_1, \lambda'_2} A_{\lambda, \lambda'_1, \lambda'_2} f_{\text{SO}}^\lambda(\mathbf{a}) f_{\text{USp}}^{\lambda'_1}(\mathbf{b}_1) f_{\text{USp}}^{\lambda'_2}(\mathbf{b}_2) , \quad (3.22)$$

$$\mathcal{I}(\mathbf{a}) = \sum_{\lambda} E_\lambda f_{\text{SO}}^\lambda(\mathbf{a}) , \quad (3.23)$$

respectively. The S-duality shown in figure 6b written in terms of the structure constants reads

$$\sum_{\lambda_1} C_{\lambda_1, \lambda'_1} B_{\lambda_1, \lambda_2, \lambda_3} = \sum_{\lambda'_2} A_{\lambda_2, \lambda'_1, \lambda'_2} C_{\lambda_3, \lambda'_2} . \quad (3.24)$$

Using the “diagonality” of $C_{\lambda, \lambda'}$ and $B_{\lambda_1, \lambda_2, \lambda_3}$ this implies that

$$C_{\lambda_1=\lambda'_1, \lambda'_1} B_{\lambda_1=\lambda'_1, \lambda_2, \lambda_3} \hat{\delta}_{\lambda_2, \lambda'_1} \hat{\delta}_{\lambda_3, \lambda'_1} = A_{\lambda_2, \lambda'_1, \lambda'_3} C_{\lambda_3=\lambda'_3, \lambda'_3} \hat{\delta}_{\lambda_3, \lambda'_3} . \quad (3.25)$$

Here we used the shorthand notation that $\lambda = \lambda'$ means $\lambda = (\lambda'_1, \dots, \lambda'_{n-1}, \lambda'_{n-1})$ and $\hat{\delta}_{\lambda, \lambda'}$ imposes the same condition. Now we find that $A_{\lambda_2, \lambda'_1, \lambda'_3}$ vanishes unless $\lambda'_1 = \lambda'_3$ and $\lambda_2 = \lambda'_1$. This relation also fixes the value of the A structure constants as

$$A_{\lambda, \lambda'_1, \lambda'_2} = \hat{\delta}_{\lambda, \lambda'_1} \delta_{\lambda'_1, \lambda'_2} B_{\lambda_1=\lambda'_1, \lambda_2=\lambda'_1, \lambda_3=\lambda'_1} . \quad (3.26)$$

⁷This would follow at once from the approach of [15], namely if one could derive the action of D on the index of theory \mathcal{T} by extracting residues (in flavor fugacities) in the index of a bigger theory \mathcal{T}' . Taking residues in different duality frames of \mathcal{T}' one would get the action of D on different flavor punctures of \mathcal{T} . Invariance of the index under S-duality would then imply diagonality in the basis of the eigenfunctions of D . As in [15], we also expect that acting with D on the index amounts to decorating the $4d$ theory with a BPS surface defect.

The “diagonality” of the A structure constants means that the sum in equation (3.22) runs only over $\mathrm{USp}(2n-2)$ representations.

A similar reasoning will allow us to obtain the E structure constants from the S-duality in figure 6a, which reads

$$\sum_{\lambda'} C_{\lambda_2, \lambda'} C_{\lambda_3, \lambda'} = \sum_{\lambda_1} B_{\lambda_1, \lambda_2, \lambda_3} E_{\lambda_1}. \quad (3.27)$$

The “diagonality” of C and B implies that E_λ will vanish unless it is of the form $\lambda = (\lambda_1, \dots, \lambda_{n-1}, \lambda_{n-1})$, and so the sum in equation (3.23) does not run over all $\mathrm{SO}(2n)$ representations. The value of E is also fixed by this duality to be

$$E_\lambda = \hat{\delta}_{\lambda=\lambda'} \frac{C_{\lambda=\lambda', \lambda'}^2}{B_{\lambda_1=\lambda', \lambda_2=\lambda', \lambda_3=\lambda'}}. \quad (3.28)$$

Having introduced the structure constants for the different basic spheres, we now turn to evaluating them in some special cases. In our calculations we have made extensive use of the LieART Mathematica package of [28], and use the determinantal formula of [29] to compute the Macdonald polynomials.

3.3 D_2 theories

Although not an honest member of the D -series, we will start our discussion of the structure constants with $D_2 \equiv A_1 \times A_1$. Due to the low rank, it is possible to obtain exact results in the Hall-Littlewood and Schur limits. These theories also allow for an interesting interpretation in terms of A_1 theories.

3.3.1 Hall-Littlewood limit

The simplest limit of enhanced supersymmetry is the Hall-Littlewood limit, *i.e.* $p \rightarrow 0, q \rightarrow 0$, since then the q -Pochhammer symbols in equations (3.8)-(3.10) simplify, as $(x; 0)_\infty = 1 - x$. Moreover, all sums over representations will be geometric progressions.

Without much ado, we write the index of the free hypermultiplet for the D_2 theory as

$$\mathcal{I}(\mathbf{a}, b) = \mathcal{A}(\tau) \sum_{\lambda'=0}^{\infty} \frac{\mathcal{K}_{\mathrm{USp}}(\times) P_{HL\mathrm{USp}}^{(\lambda')}(\tau | \tau) \mathcal{K}_{\mathrm{USp}}(b) P_{HL\mathrm{USp}}^{(\lambda')}(b | \tau) \mathcal{K}_{\mathrm{SO}}(\mathbf{a}) P_{HLSO}^{(\lambda', \lambda')}(\mathbf{a} | \tau)}{P_{HLSO}^{(\lambda', \lambda')}(1, \tau^2 | \tau)}, \quad (3.29)$$

where we defined

$$\mathcal{K}_{\mathrm{USp}}(\times) = \frac{\sqrt{1-\tau^2}}{1-\tau^4}, \quad \mathcal{A}(\tau) = \frac{(1-\tau^4)^2}{1-\tau^2}. \quad (3.30)$$

The equality of the above expression with equation (3.10) for $q = 0$ was checked by performing the sum over representations, which is geometric. We can read off the structure constant $C_{\lambda=\lambda', \lambda'}$ to be

$$C_{\lambda=\lambda', \lambda'} = \frac{\mathcal{A}(\tau) \mathcal{K}_{\mathrm{USp}}(\times) P_{HL\mathrm{USp}}^{(\lambda')}(\tau | \tau)}{\dim_{\tau^2}^{\mathrm{SO}}(\lambda = \lambda')}, \quad (3.31)$$

where we used the Hall-Littlewood limit of the $\text{SO}(4)$ (q, t) -dimension formula.

In general, the (q, t) -dimension (or Macdonald dimension) for $\text{SO}(2n)$ is given by

$$\dim_{q,t}^{\text{SO}}(\lambda) = P_{M\text{SO}}^\lambda(1, t, \dots, t^{n-1} \mid q, t). \quad (3.32)$$

The usual limits apply: $q \rightarrow 0$ gives the Hall-Littlewood or t -dimension \dim_t^{SO} and $q = t$ gives the Schur dimension \dim_q^{SO} , also known as the q -dimension. In the Hall-Littlewood limit we write $t = \tau^2$.

The expression (3.31) for the structure constant, as well as the ones below for the other spheres, will hold in the other limits and for higher rank if naturally modified and generalized.

Since $\text{USp}(2) = \text{SU}(2)$, we can apply the procedure of [15] to close the $\text{USp}(2)$ puncture and obtain the index of the sphere with one $\text{SO}(4)$ puncture and two closed USp punctures. This index is computed as $2 \mathcal{I}_V \text{Res}_{b=\tau}(\frac{1}{b} \mathcal{I}(\mathbf{a}, b))$, with $\mathcal{I}_V = \text{PE}[f_V]$. We find

$$\mathcal{I}(\mathbf{a}) = \mathcal{A}(\tau) \sum_{\lambda'=0}^{\infty} \frac{\left(\mathcal{K}_{\text{USp}}(\times) P_{HL\text{USp}}^{(\lambda')}(\tau \mid \tau) \right)^2 \mathcal{K}_{\text{SO}}(\mathbf{a}) P_{HL\text{SO}}^{(\lambda', \lambda')}(\mathbf{a} \mid \tau)}{P_{HL\text{SO}}^{(\lambda', \lambda')}(1, \tau^2 \mid \tau)}. \quad (3.33)$$

Notice that the index for this sphere vanishes when summed over representations. Since it has $n_V = -3$ and $n_H = 0$ it only makes sense as part of a larger theory, *e.g.* in figure 6a. The E_λ structure constant is

$$E_{\lambda=\lambda'} = \frac{\mathcal{A}(\tau) \mathcal{K}_{\text{USp}}(\times) P_{HL\text{USp}}^{(\lambda')}(\tau \mid \tau) \mathcal{K}_{\text{USp}}(\times) P_{HL\text{USp}}^{(\lambda')}(\tau \mid \tau)}{\dim_{\tau^2}^{\text{SO}}(\lambda = \lambda')}. \quad (3.34)$$

Considering the relations imposed by S-duality in (3.28) and (3.26) one can now also write down the index for the $T_{\text{SO}(4)}$ theory and the $\tilde{T}_{\text{SO}(4)}$ theory, respectively, as

$$\mathcal{I}_{T_{\text{SO}(4)}}(\mathbf{a}_1, \mathbf{a}_2, \mathbf{a}_3) = \mathcal{A}(\tau) \sum_{\lambda_1, \lambda_2=0}^{\infty} \frac{1}{P_{HL\text{SO}}^{(\lambda_1, \lambda_2)}(1, \tau^2 \mid \tau)} \prod_{i=1}^3 \mathcal{K}_{\text{SO}}(\mathbf{a}_i) P_{HL\text{SO}}^{(\lambda_1, \lambda_2)}(\mathbf{a}_i \mid \tau) \quad (3.35)$$

and

$$\mathcal{I}_{\tilde{T}_{\text{SO}(4)}}(\mathbf{a}, b_1, b_2) = \mathcal{A}(\tau) \sum_{\lambda'=0}^{\infty} \frac{\mathcal{K}_{\text{SO}}(\mathbf{a}) P_{HL\text{SO}}^{(\lambda', \lambda')}(\mathbf{a} \mid \tau) \prod_{i=1}^2 \mathcal{K}_{\text{USp}}(b_i) P_{HL\text{USp}}^{(\lambda')}(b_i \mid \tau)}{P_{HL\text{SO}}^{(\lambda', \lambda')}(1, \tau^2 \mid \tau)}. \quad (3.36)$$

These results were also checked against the construction in figure 3 and 4. The index for the linear quivers was expanded in powers of τ and compared to the expansion of the $T_{\text{SO}(4)}$ (respectively $\tilde{T}_{\text{SO}(4)}$) theory glued to its three tails. On the other hand, the independent construction of the $T_{\text{SO}(4)}$ and $\tilde{T}_{\text{SO}(4)}$ provides evidence of the S-duality in figure 6b. The structure constants for these theories are

$$B_{\lambda, \lambda, \lambda} = \frac{\mathcal{A}(\tau)}{\dim_{\tau^2}^{\text{SO}}(\lambda)}, \quad A_{\lambda=\lambda', \lambda', \lambda'} = \frac{\mathcal{A}(\tau)}{\dim_{\tau^2}^{\text{SO}}(\lambda = \lambda')}. \quad (3.37)$$

For the $T_{\text{SO}(4)}$ theory, we recall that, from equation (2.1), the effective number of hypermultiplets in this theory is 8, and the effective number of vectormultiplets is 0. In fact,

we claim that it corresponds to the index of one half-hypermultiplet in the $\mathbf{2} \times \mathbf{2} \times \mathbf{2}$ and another in the $\bar{\mathbf{2}} \times \bar{\mathbf{2}} \times \bar{\mathbf{2}}$ of the flavor symmetry group $\text{SO}(4)^3$. This was checked in a τ expansion, and numerically after performing the sum over representations. We will discuss this further in Sec. 3.3.4.

3.3.2 Schur limit

The index for the free half-hypermultiplet in the Schur limit is given by

$$\mathcal{I}(\mathbf{a}, b) = \mathcal{A}(q) \sum_{\lambda'=0}^{\infty} \frac{\mathcal{K}_{\text{USp}}(\times) \chi_{\text{USp}}^{(\lambda')} (q^{1/2}) \mathcal{K}_{\text{USp}}(b) \chi_{\text{USp}}^{(\lambda')} (b) \mathcal{K}_{\text{SO}}(\mathbf{a}) \chi_{\text{SO}}^{(\lambda', \lambda')} (\mathbf{a})}{\chi_{\text{SO}}^{(\lambda', \lambda')} (1, q)}, \quad (3.38)$$

where we define

$$\mathcal{K}_{\text{USp}}(\times) = \frac{1}{(q^2; q)}, \quad \mathcal{A}(q) = (q^2; q)_{\infty}^2. \quad (3.39)$$

The equality of the above expression with equation (3.10) for $q = t$ was proved exactly by comparing the analytic structure of both sides. In fact, as we will see later in Sec. 3.3.4, a redefinition of the fugacities maps this theory onto the T_2 theory discussed in [14], and therefore the proof is immediate from the similar proof there.

The index of the $T_{\text{SO}(4)}$ theory is

$$\mathcal{I}_{T_{\text{SO}(4)}}(\mathbf{a}_1, \mathbf{a}_2, \mathbf{a}_3) = \mathcal{A}(q) \sum_{\lambda_1, \lambda_2=0}^{\infty} \frac{1}{\chi_{\text{SO}}^{(\lambda_1, \lambda_2)} (1, q)} \prod_{i=1}^3 \mathcal{K}_{\text{SO}}(\mathbf{a}_i) \chi_{\text{SO}}^{(\lambda_1, \lambda_2)} (\mathbf{a}_i). \quad (3.40)$$

Again we checked this expression using the construction of figure 3 by expanding the index for both sides in q . S-duality then fixes the index for the other three-punctured spheres. The index for $\tilde{T}_{\text{SO}(4)}$ was independently checked against the construction of figure 4 in a q expansion.

3.3.3 Macdonald limit

Let us finally state our claim in the Macdonald limit. For the free half-hypermultiplet we have

$$\begin{aligned} \mathcal{I}(\mathbf{a}, b) &= \\ \mathcal{A}(q, t) \sum_{\lambda'} \frac{\mathcal{K}_{\text{USp}}(\times) P_{M\text{USp}}^{(\lambda')} (t^{1/2} | q, t) \mathcal{K}_{\text{USp}}(b) P_{M\text{USp}}^{(\lambda')} (b | q, t) \mathcal{K}_{\text{SO}}(\mathbf{a}) P_{M\text{SO}}^{(\lambda', \lambda')} (\mathbf{a} | q, t)}{P_{M\text{SO}}^{(\lambda', \lambda')} (1, t | q, t)}, \\ \mathcal{A}(q, t) &= (t^2; q)_{\infty}^2 \left(\frac{(q; q)_{\infty}}{(t; q)_{\infty}} \right), \quad \mathcal{K}_{\text{USp}}(\times) = \left(\frac{(t; q)_{\infty}}{(q; q)_{\infty}} \right)^{\frac{1}{2}} (t^2; q)_{\infty}^{-1}. \end{aligned} \quad (3.41)$$

Some of the structure constants were computed in an expansion in q and t , and the equality was also checked numerically, truncating the sum at high enough λ' .

For the $T_{\text{SO}(4)}$ theory we have

$$\mathcal{I}_{T_{\text{SO}(4)}}(\mathbf{a}_1, \mathbf{a}_2, \mathbf{a}_3) = \sum_{\lambda_1, \lambda_2} \frac{\mathcal{A}(q, t)}{P_{M\text{SO}}^{(\lambda_1, \lambda_2)} (1, t | q, t)} \prod_{i=1}^3 \mathcal{K}_{\text{SO}}(\mathbf{a}_i) P_{M\text{SO}}^{(\lambda_1, \lambda_2)} (\mathbf{a}_i | q, t),$$

where the sum runs over all $\text{SO}(4)$ representations.

3.3.4 D_2 theories in terms of A_1 theories

Since locally $\mathrm{SO}(4) = \mathrm{SU}(2) \times \mathrm{SU}(2)$, $\mathrm{USp}(2) = \mathrm{SU}(2)$ and in the superconformal tails $\mathrm{SO}(3) = \mathrm{SU}(2)$, one expects that the D_2 theories can also be described in terms of the A_1 theory [7].

As mentioned before, one naturally considers alternating quivers (see also section 4.1), which for D_2 theories have gauge groups

$$\mathrm{SO}(3) \times \mathrm{USp}(2) \times \mathrm{SO}(4) \times \dots \times \mathrm{USp}(2) \times \mathrm{SO}(3). \quad (3.42)$$

Calling the number of $\mathrm{SO}(4)$ gauge groups s , the corresponding Riemann surface is a sphere with $2s + 6$ empty $\mathrm{USp}(2)$ punctures \times connected in pairs by $s + 3$ twist lines. In A_1 language, it corresponds to a genus $s + 2$ Riemann surface, which however, since the couplings of the two $\mathrm{SU}(2)$ s within $\mathrm{SO}(4)$ are not independent, is hyperelliptic [7].

In writing $\mathrm{SO}(4)$ as the product of two $\mathrm{SU}(2)$ s, the Macdonald polynomials decompose as

$$P_{M\mathrm{SO}}^{(\lambda_1, \lambda_2)}(a_1, a_2 \mid q, t) = P_{M\mathrm{SU}}^{(\lambda_1)}\left(\sqrt{\frac{a_1}{a_2}}, \sqrt{\frac{a_2}{a_1}} \mid q, t\right) P_{M\mathrm{SU}}^{(\lambda_2)}\left(\sqrt{a_1 a_2}, \frac{1}{\sqrt{a_1 a_2}} \mid q, t\right). \quad (3.43)$$

As a consequence, an $\mathrm{SO}(4)$ puncture splits into two $\mathrm{SU}(2)$ punctures, and the $\mathrm{SO}(4)$ propagator turns into two $\mathrm{SU}(2)$ propagators connecting the two $\mathrm{SU}(2)$ punctures separately.

Let us now rewrite the index for the basic D_2 spheres in terms of A_1 quantities. First, we have that the index of the free D_2 half-hypermultiplet \mathcal{I}_{D_2} trivially equals the index of the T_2 theory \mathcal{I}_{T_2} if the fugacities are appropriately identified:

$$\mathcal{I}_{D_2}((a_1, a_2), b) = \mathcal{I}_{T_2}\left(\sqrt{a_1 a_2}, \sqrt{\frac{a_1}{a_2}}, b\right). \quad (3.44)$$

Second, the index for the $T_{\mathrm{SO}(4)}$ theory is, as was mentioned already, equal to the index of one half-hypermultiplet in the $\mathbf{2} \times \mathbf{2} \times \mathbf{2}$ and another in the $\bar{\mathbf{2}} \times \bar{\mathbf{2}} \times \bar{\mathbf{2}}$ of the flavor symmetry group $\mathrm{SO}(4)^3$. This can be rewritten in terms of a product of indices of the T_2 theory.

$$\begin{aligned} \mathcal{I}_{T_{\mathrm{SO}(4)}}((a_1, a_2), (A_1, A_2), (\alpha_1, \alpha_2)) = \\ \mathcal{I}_{T_2}\left(\sqrt{a_1 a_2}, \sqrt{A_1 A_2}, \sqrt{\alpha_1 \alpha_2}\right) \mathcal{I}_{T_2}\left(\sqrt{\frac{a_1}{a_2}}, \sqrt{\frac{A_1}{A_2}}, \sqrt{\frac{\alpha_1}{\alpha_2}}\right). \end{aligned} \quad (3.45)$$

This factorized expression can also be easily checked by applying (3.43) to the expression for the index in (3.42) and noticing that the \mathcal{K} -factors and \mathcal{A} decompose nicely in the product of the corresponding $\mathrm{SU}(2)$ quantities. The result (3.45) can be understood from the construction of the $T_{\mathrm{SO}(4)}$ theory in figure 3. Here we have the three-punctured sphere with three maximal $\mathrm{SO}(4)$ punctures, of which from each the diagonal $\mathrm{SO}(3)$ subgroup is gauged. The curve corresponding to the linear quiver describing this theory is a sphere with six empty USp punctures \times . The corresponding A_1 hyperelliptic curve is a genus two surface, which can be thought of as gluing together two three-punctured spheres. One can now observe that each of these three-punctured spheres contains one of the two $\mathrm{SU}(2)$

punctures in which each of the three $\text{SO}(4)$ punctures split and gauging the diagonal $\text{SO}(3)$ subgroup is indeed obtained by gluing these together.

Third, the index for the $\tilde{T}_{\text{SO}(4)}$ theory is equal to the A_1 index of the four-punctured sphere if again the $\text{SO}(4)$ fugacities are appropriately identified,

$$\mathcal{I}_{\tilde{T}_{\text{SO}(4)}}((a_1, a_2), b, c) = \mathcal{I}_{4\text{-punctured}}^{\text{SU}(2)}\left(\sqrt{a_1 a_2}, \sqrt{\frac{a_1}{a_2}}, b, c\right). \quad (3.46)$$

Notice that the number of effective hyper and vectormultiplets is the same for both theories, as can be inferred from (2.2), namely eight and three respectively. We can also understand the result (3.46) from the construction in figure 4. There we have the three-punctured sphere with one maximal $\text{SO}(4)$ puncture, of which the diagonal $\text{SO}(3)$ subgroup is gauged, and two maximal $\text{USp}(2)$ punctures, which each are connected to an $\text{SO}(3)$ gauge group. The linear quiver describing this theory corresponds to a sphere with eight empty USp punctures \times , and the corresponding A_1 hyperelliptic curve is a genus three surface. This surface can be thought of as originating from a four-punctured sphere of which two punctures are glued to each other and the two other punctures are glued to a torus. As before, gluing the two punctures to each other corresponds to gauging the diagonal $\text{SO}(3)$ subgroup, and gluing a torus corresponds to connecting to an $\text{SO}(3)$ gauge group (since the adjoint of $\text{SO}(3)$ equals the adjoint of $\text{SU}(2)$).

Finally, one can also interpret the partially closed colored box-shaped $\text{SO}(4)$ puncture in A_1 language. We will do so in section 4.2.2.

3.4 D_3 theories

We claim that in the D_3 case the index of the free hypermultiplet is given by

$$\begin{aligned} \mathcal{I}(\mathbf{a}, \mathbf{b}) &= \\ \mathcal{A}(q, t) \sum_{\lambda} \frac{\mathcal{K}_{\text{USp}}(\times) P_{M \text{USp}}^{\lambda'}(t^{1/2}, t^{3/2} | q, t) \mathcal{K}_{\text{USp}}(\mathbf{b}) P_{M \text{USp}}^{\lambda'}(\mathbf{b} | q, t) \mathcal{K}_{\text{SO}}(\mathbf{a}) P_{M \text{SO}}^{\lambda=\lambda'}(\mathbf{a} | q, t)}{P_{M \text{SO}}^{\lambda=\lambda'}(1, t, t^2 | q, t)}, \\ \mathcal{A}(q, t) &= (t^3; q)_{\infty} \left(\frac{(q; q)_{\infty}}{(t; q)_{\infty}} \right)^{3/2} \prod_{l=1}^2 (t^{2l}; q)_{\infty}, \\ \mathcal{K}_{\text{USp}}(\times) &= \frac{(t; q)_{\infty}}{(q; q)_{\infty}} \prod_{l=1}^2 (t^{2l}; q)_{\infty}^{-1}. \end{aligned} \quad (3.47)$$

In the Hall-Littlewood limit this equality was checked numerically after performing the sum exactly. In the Schur limit these coefficients were checked in a q expansion for several representations, and the equality of the index in this limit was also checked numerically, truncating the sum over representations at a high enough λ' .

Since $\text{SO}(6) = \text{SU}(4)$, the $T_{\text{SO}(6)}$ theory is the same as the T_4 theory (the sphere with 3 maximal $\text{SU}(4)$ punctures), the index of which was computed in [14]. The index for this theory can then just be found from equation (7.11) of [14] by re-writing the $\text{SU}(4)$ Macdonald polynomials as $\text{SO}(6)$ polynomials. Denoting the $\text{SU}(4)$ fugacities by (c_1, c_2, c_3, c_4) , subject to the constraint $c_1 c_2 c_3 c_4 = 1$, we have $P_{M \text{SU}}^{\lambda}(c_1, c_2, c_3, c_4) = P_{M \text{SO}}^{\lambda}(c_1 c_2, c_1 c_3, c_2 c_3)$,

where $\tilde{\lambda}$ denotes the $\text{SU}(4)$ representation corresponding to the λ $\text{SO}(6)$ representation. The index then becomes, with the sum running over all $\text{SO}(6)$ representations,

$$\mathcal{I}_{T_{\text{SO}(6)}}(\mathbf{a}_1, \mathbf{a}_2, \mathbf{a}_3) = \sum_{\lambda} \frac{\mathcal{A}(q, t)}{P_{M\text{SO}}^{\lambda}(1, t, t^2 | q, t)} \prod_{i=1}^3 \mathcal{K}_{\text{SO}}(\mathbf{a}_i) P_{M\text{SO}}^{\lambda}(\mathbf{a}_i | q, t) .$$

S-duality then fixes the index of the $\tilde{T}_{\text{SO}(6)}$, and as in the D_2 case this index was independently checked using the construction of figure 4 both in the Hall-Littlewood and Schur limits (in a τ and q expansion respectively).

3.5 D_n theories

Let us finally state our conjecture for the D_n theory in the Macdonald limit⁸. The index associated to the free hypermultiplet in the bifundamental of $\text{SO}(2n) \times \text{USp}(2n-2)$ is

$$\begin{aligned} \mathcal{I}(\mathbf{a}, \mathbf{b}) &= \sum_{\lambda} \frac{\mathcal{A}(q, t)}{P_{M\text{SO}}^{\lambda=\lambda'}(1, t, \dots, t^{n-1} | q, t)} \mathcal{K}_{\text{USp}}(\times) P_{M\text{USp}}^{\lambda'}(t^{1/2}, t^{3/2}, \dots, t^{n-3/2} | q, t) \times \\ &\quad \times \mathcal{K}_{\text{USp}}(\mathbf{b}) P_{M\text{USp}}^{\lambda'}(\mathbf{b} | q, t) \mathcal{K}_{\text{SO}}(\mathbf{a}) P_{M\text{SO}}^{\lambda=\lambda'}(\mathbf{a} | q, t) , \\ \mathcal{A}(q, t) &= (t^n; q)_{\infty} \left(\frac{(q; q)_{\infty}}{(t; q)_{\infty}} \right)^{n/2} \prod_{l=1}^{n-1} (t^{2l}; q)_{\infty} , \\ \mathcal{K}_{\text{USp}}(\times) &= \left(\frac{(t; q)_{\infty}}{(q; q)_{\infty}} \right)^{\frac{n-1}{2}} \prod_{l=1}^{n-1} (t^{2l}; q)_{\infty}^{-1} . \end{aligned} \tag{3.48}$$

This expression was checked numerically for D_4 in the Hall-Littlewood and Schur limits by truncating the sum over representations. For the $T_{\text{SO}(2n)}$ theory we conjecture

$$\mathcal{I}_{T_{\text{SO}(2n)}}(\mathbf{a}_1, \mathbf{a}_2, \mathbf{a}_3) = \sum_{\lambda} \frac{\mathcal{A}(q, t)}{P_{M\text{SO}}^{\lambda}(1, t, \dots, t^{n-1} | q, t)} \prod_{i=1}^3 \mathcal{K}_{\text{SO}}(\mathbf{a}_i) P_{M\text{SO}}^{\lambda}(\mathbf{a}_i | q, t) ,$$

where the sum runs over all $\text{SO}(2n)$ representations. The genus g partition function for the pure $\text{SO}(2n)$ theory is

$$\begin{aligned} \mathcal{I}_{T_{\text{SO}(2n)}} &= \sum_{\lambda} \left(\frac{\mathcal{A}(q, t)}{\dim_{q,t}^{\text{SO}}(\lambda)} \right)^{2g-2} \\ &= ((q; q)_{\infty} (t; q)_{\infty})^{n(g-1)} \left(\frac{(t; q)_{\infty}}{(t^n; q)_{\infty}} \prod_{l=1}^{n-1} \frac{(t; q)_{\infty}}{(t^{2l}; q)_{\infty}} \right)^{2-2g} \sum_{\lambda} \frac{1}{(\dim_{q,t}^{\text{SO}}(\lambda))^{2g-2}} . \end{aligned} \tag{3.49}$$

As in [14], for the slice $t = q^{\beta}$ this result appears to be related to the partition function $Z(\mathcal{C} \times S^1)$ of a refinement of level k Chern-Simons theory discussed in [30]. For a genus g Riemann surface, \mathcal{C} , Z is given by

$$Z(\mathcal{C} \times S^1) = \sum_{\lambda} \frac{1}{(S_{0\lambda})^{2g-2}}, \tag{3.50}$$

⁸Note that the \mathbb{Z}_3 outer-automorphism of D_4 allows for a richer structure, see [8]. We will not consider this \mathbb{Z}_3 twist here.

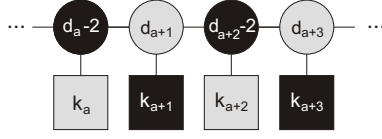


Figure 7: Generic alternating quiver.

where $S_{0\lambda}$ is given by

$$S_{0\lambda} = S_{00} \dim_{q,t}^{\text{SO}}(\lambda), \quad (3.51)$$

and S_{00} by⁹

$$S_{00} = \prod_{m=0}^{\beta-1} \prod_{\alpha > 0} \left(1 - q^m t^{\langle \alpha, \rho \rangle} \right). \quad (3.53)$$

The parameters q, t are identified as $q = \exp\left(\frac{2\pi i}{k+\beta y}\right)$ and $t = \exp\left(\frac{2\pi i \beta}{k+\beta y}\right)$. Also note that we consider the Macdonald polynomials to be normalized, and so $\dim_{q,t}^{\text{SO}}(\lambda)$ here is $\dim_{q,t}^{\text{SO}}(\lambda)/\sqrt{g_\lambda}$ in [30], where g_λ denotes the norm of the polynomials there. It is now easy to verify that our result coincides with this partition function, up to the overall factor $((q; q)_\infty (t; q)_\infty)^{n(g-1)}$.

4. Partially Closed Punctures

In this section we discuss more general theories with partially closed punctures.

4.1 Classification

The classification of superconformal tails for type D theories was discussed in [7]. Let us briefly summarize the main points. One naturally considers an alternating quiver of SO and USp gauge groups as in figure 7. In such a quiver, the requirement that every coupling is marginal implies that

$$k_a = 2d_a - d_{a+1} - d_{a-1} = (d_a - d_{a-1}) - (d_{a+1} - d_a). \quad (4.1)$$

⁹Following [14] we only kept the interesting q and t dependent part of S_{00} (see also equation (7.5) of [30]). The full three-sphere partition function is

$$S_{00} = i^{|\Delta_+|} |P/Q|^{-1/2} (k + \beta y)^{-n/2} q^{-\beta(\beta-1)|\Delta_+|/4} t^{-\beta\langle \rho, \rho \rangle} \prod_{m=0}^{\beta-1} \prod_{\alpha > 0} \left(1 - q^m t^{\langle \alpha, \rho \rangle} \right), \quad (3.52)$$

where $|\Delta_+|$ is the number of positive roots, y is the dual coxeter number and $|P/Q|$ denotes the number of elements in the fundamental cell of the quotient lattice P/Q . Note that with (3.52) there is an extra overall factor when comparing the partition function on $\mathcal{C} \times S^1$ with the superconformal index for the Riemann surface \mathcal{C} . This is precisely the same factor that appears when comparing the A -type index of [14] with the complete refined Chern-Simons partition function on $\mathcal{C} \times S^1$ for $\text{SU}(N)$.

Since k_a is a non-negative integer one finds that a general quiver necessarily has

$$d_1 < d_2 < \dots < d_l = \dots = d_r > d_{r+1} > \dots > d_m. \quad (4.2)$$

The part to the left of gauge group l and to the right of gauge group r are the two tails of this quiver. We denote $d_l = \dots = d_r = 2n$ and introduce $d_0 = d_{m+1} = 0$. Focusing on the right tail $2n = d_r > d_{r+1} > \dots > d_m$ and observing that from (4.1) $d_a - d_{a+1}$ is monotonically non-decreasing, we can associate a Young tableau to this quiver as follows. If the quiver ends in a USp gauge group, one considers a grey - *i.e.* SO - tableau with length of rows given by $d_r - d_{r+1}, d_{r+1} - d_{r+2}, \dots$, which has a total number of boxes of $2n$. If on the other hand the quiver ends in a SO gauge group, then one can construct a black tableau with length of rows given by $d_r - d_{r+1}, d_{r+1} - d_{r+2}, \dots, d_{m-1} - d_m, d_m - d_{m+1} - 2$, which has a total number of boxes equal to $2n - 2$.

The Young tableau thus constructed encodes as usual the embedding of $SU(2)$ in $SO(2n)$ ($USp(2n-2)$), the commutant of which captures the flavor symmetry information. The embedding is given by the decomposition of the vector representation $2n$ of $SO(2n)$ (fundamental representation $2n-2$ of $USp(2n-2)$) under $SU(2)$. Let us denote the number of columns of height h by l_h . Then the relation between the Young tableau and the decomposition is given for a grey tableau by

$$2n \rightarrow \underbrace{1 + 1 + \dots + 1}_{l_1} + \underbrace{2 + 2 + \dots + 2}_{l_2} + \dots \quad (4.3)$$

Note that the reality of the vector representation requires that l_h is even for even h . The flavor symmetry associated to such a tail is then

$$\prod_{h:\text{odd}, l_h \geq 2} SO(l_h) \times \prod_{h:\text{even}, l_h \geq 2} USp(l_h), \quad (4.4)$$

where the USp groups have an even argument indeed. Following [10] we call decompositions (4.3) in which only even dimensional representations appear “very even”. Since even dimensional representations must occur with even multiplicities, this case only occurs for even n . Actually, such tableaux correspond to two different punctures which are exchanged by the \mathbb{Z}_2 outer automorphism and were colored red and blue in [10].

Note that if the decomposition of the vector representation into $SU(2)$ representations is of the form $2n \rightarrow (2n-k) + k$ for arbitrary odd k , or $k = n$ if n even, the above algorithm will give rise to a “USp(0)” gauge group. The occurrence of such a gauge group can be understood from the brane picture, see [7].

For a black tableau one has

$$2n - 2 \rightarrow \underbrace{1 + 1 + \dots + 1}_{l_1} + \underbrace{2 + 2 + \dots + 2}_{l_2} + \dots \quad (4.5)$$

Note that the pseudo-reality of the fundamental representation requires that l_h is odd for even h . The flavor symmetry associated to such a tail is then

$$\prod_{h:\text{odd}, l_h \geq 2} USp(l_h) \times \prod_{h:\text{even}, l_h \geq 2} SO(l_h). \quad (4.6)$$

The curve corresponding to these superconformal tails has $m - r + 4$ punctures (or simply said, the number of gauge groups plus three) of which one is a maximal SO puncture, one puncture is the partially closed one under consideration and the other $m - r + 2$ punctures are empty USp punctures \times . Note that a possible “USp(0)” gauge group is also included in this counting of gauge groups.

4.2 The index with partially closed punctures

Following [14], we generalize the structure of the superconformal index in section 3.5 to include partially closed punctures. For a three punctured sphere with punctures labeled by a Young tableau Y_I we propose schematically

$$\mathcal{I} = \mathcal{A}(q, t) \sum_{\lambda} \frac{\prod_{I=1}^3 \mathcal{K}(Y_I) P_M^{\lambda}(Y_I | q, t)}{P_{M \text{ SO}}^{\lambda}(1, t, \dots, t^{n-1} | q, t)}. \quad (4.7)$$

Here the color of the Young tableau determines whether one considers SO or USp polynomials and corresponding \mathcal{K} -factors. Due to the twist line there are either no or two USp punctures. If USp punctures are present the sum is over USp representations and the occurring SO representations are restricted in the sense discussed above. The denominator is always the (q, t) - dimension of type SO.

Given this structure, we need to determine for each allowed Young tableau which fugacities one needs to plug in the polynomials and what the \mathcal{K} -factor associated to that puncture is.

4.2.1 Fugacities corresponding to Young diagram

To find which fugacities appropriately describe a partially closed puncture we use that a partially closed $\text{SO}(2n)$ ($\text{USp}(2n - 2)$) puncture is classified by an embedding of $\text{SU}(2)$ determined by the decomposition of the vector (fundamental) representation of this group and that the multiplicities with which the different $\text{SU}(2)$ representations occur encode the corresponding flavor symmetry. The fugacities are correspondingly determined by looking at the following equality. On one side of the equality, one simply writes the character of the vector (fundamental) representation in terms of its n ($n - 1$) fugacities. On the other side of the equality we write the decomposition determined by the puncture in $\text{SU}(2)$ characters with as $\text{SU}(2)$ fugacity $\tau = t^{1/2}$, where we replace the multiplicities by the character of the vector/fundamental of the flavor symmetry determined by that multiplicity. One can now simply read off the relevant fugacities. How one identifies the fugacities does not matter in USp, *i.e.* neither the order nor if one chooses X or X^{-1} is relevant, because these operations precisely correspond to Weyl symmetries, under which the Macdonald polynomials are invariant. For the SO punctures, the order of the fugacities again corresponds to a Weyl symmetry. However, in this case Weyl invariance only means we can invert fugacities in pairs. For odd rank, the tableau always contains at least two columns of odd height. This implies that the two apparently different choices one obtains after exploiting the Weyl symmetries correspond to a renaming of the fugacities. For even rank, there also are odd height columns if the decomposition is not “very even”. Then again, there is a unique

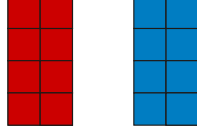


Figure 8: An example of a “very even” $\text{SO}(8)$ puncture with $\text{USp}(2)$ flavor symmetry. We write $\sum_{i=1}^4 a_i + a_i^{-1} = (\tau^3 + \tau + \tau^{-1} + \tau^{-3})(b + 1/b)$, where b is the $\text{USp}(2)$ fugacity. The two essentially inequivalent choices are $a_1 = b\tau^3, a_2 = b\tau, a_3 = b\tau, a_4 = b/\tau^3$, and $a_1 = b\tau^3, a_2 = b\tau, a_3 = b\tau, a_4 = \tau^3/b$. They correspond to the red and blue punctures respectively.¹⁰

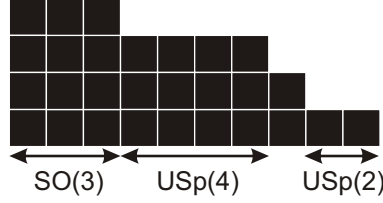


Figure 9: $\text{USp}(28)$ puncture with $\text{SO}(3) \times \text{USp}(4) \times \text{USp}(2)$ flavor symmetry.

choice of fugacities up to a renaming. However, for the “very even” case, there are two essentially inequivalent choices. These are interchanged by the \mathbb{Z}_2 outer-automorphism, and they correspond to the red and blue punctures. We illustrate this in figure 8. This distinction disappears once one considers the puncture as part of a Riemann surface containing also USp punctures, since then the sum over $\text{SO}(2n)$ representations is restricted due to “diagonality”, *i.e.* only representations for which the last orthogonal weight is zero ($\ell_n = 0$) appear. In this case inverting any fugacity becomes a symmetry of the polynomial.

For example, consider the $\text{USp}(28)$ puncture depicted in figure 9, the flavor symmetry is $\text{SO}(3) \times \text{USp}(4) \times \text{USp}(2)$. Then we write

$$\begin{aligned} \sum_{\alpha=1}^{14} \left(b_{\alpha} + \frac{1}{b_{\alpha}} \right) &= (\tau^3 + \tau + \tau^{-1} + \tau^{-3}) \left(a + \frac{1}{a} + 1 \right) \\ &+ (\tau^2 + 1 + \tau^{-2}) \left(\beta_1 + \frac{1}{\beta_1} + \beta_2 + \frac{1}{\beta_2} \right) \\ &+ (\tau + \tau^{-1}) \cdot 1 + 1 \cdot \left(\gamma + \frac{1}{\gamma} \right), \end{aligned} \quad (4.8)$$

where a is an $\text{SO}(3)$ fugacity, β_1, β_2 are $\text{USp}(4)$ fugacities and γ is a $\text{USp}(2)$ fugacity and one takes for example $b_1 = a\tau^3, b_2 = a\tau, b_3 = a\tau^{-1}, b_4 = a\tau^{-3}, b_5 = \tau^3, b_6 = \tau, b_7 = \beta_1\tau^2, b_8 = \beta_1, b_9 = \beta_1\tau^{-2}, b_{10} = \beta_2\tau^2, b_{11} = \beta_2, b_{12} = \beta_2\tau^{-2}, b_{13} = \tau, b_{14} = \gamma$.

¹⁰We checked this assignment by computing the ratio of the index of a free half-hypermultiplet in representation $(1, 4, 8_s) + (2, 1, 8_c)$ of the flavor symmetry group $\text{USp}(2) \times \text{USp}(4) \times \text{SO}(8)$ and the index of a free half-hypermultiplet in representation $(1, 4, 8_c) + (2, 1, 8_s)$ [10], in a τ expansion in the Hall-Littlewood limit.

4.2.2 \mathcal{K} -factors

We now turn attention to the \mathcal{K} -factors, which are independent of the red and blue coloring. For a general maximal puncture, the \mathcal{K} -factor is given in (3.16) in terms of the roots. For the empty USp puncture \times , the \mathcal{K} -factor was given in general in (3.48). For the L-shaped empty SO puncture, one can easily find the \mathcal{K} -factor by demanding that one obtains the propagator by closing one puncture in T_{SO} . The resulting \mathcal{K} -factor is then

$$\mathcal{K} \left(\begin{array}{c} \blacksquare \\ \blacksquare \\ \vdots \\ \blacksquare \\ \blacksquare \end{array} \right) = \frac{1}{\mathcal{A}(q, t)} \quad (4.9)$$

Note that in general, there are more punctures in both SO and USp which do not carry flavor symmetry. All of these factors can be determined by the following procedure.

As was discussed above, each puncture is constructed as a certain superconformal tail and as such is naturally associated to a certain Riemann surface. By comparing the index of the tail, which is straightforward to write down since it is Lagrangian, with the index of the Riemann surface associated to it, one can fix, in principle, all $\mathcal{K}(Y_I)$.

The index of a Riemann surface of genus g and with s punctures, labeled by Young tableaux Y_I is given by

$$\mathcal{I}_{g,s} = \sum_{\lambda} \left(\frac{\mathcal{A}(q, t)}{\dim_{q,t}^{\text{SO}}(\lambda)} \right)^{2g-2+s} \prod_{I=1}^s \mathcal{K}(Y_I) P_M^{\lambda}(Y_I | q, t) . \quad (4.10)$$

As before, the color of the Y_I encodes whether the Macdonald polynomials correspond to SO or USp groups. Here the sum over λ is restricted as soon as USp punctures appear, or there is a twist line wrapping an a -cycle. Riemann surfaces associated to partially closed punctures have genus zero, one maximal SO puncture, several empty USp punctures and the partially closed puncture itself.

To implement the above construction, it is convenient to consider a general Ansatz for the \mathcal{K} -factors, as follows. The \mathcal{K} -factor for the maximal puncture diverges if one plugs in the fugacities associated to a non-maximal Young tableau. However, from [15, 31] we expect to obtain the \mathcal{K} -factor associated with a Young tableau from \mathcal{K} for the maximal puncture by removing some factors, including the divergent ones, and multiplying by an appropriate power of $\mathcal{I}^V = (t; q)_{\infty}(q; q)_{\infty}$. Taking out the divergent factors, and allowing for an extra arbitrary power of $(t; q)_{\infty}(q; q)_{\infty}$ thus provides an Ansatz for each $\mathcal{K}(Y_I)$, and one can determine which terms must be removed by comparing the index of the superconformal tail described above to the corresponding Riemann surface.

Equipped with a general recipe, it would be interesting to check the dualities of [32] by comparing the index in different frames, especially for the cases where enhanced flavor symmetries appear.

We now discuss some simple examples.

D_3 theory. For the D_3 theory all the \mathcal{K} -factors for SO punctures are known from the corresponding SU(4) punctures, if one appropriately identifies the fugacities corresponding to the reduced flavor symmetries. Using the above procedure, these results were also

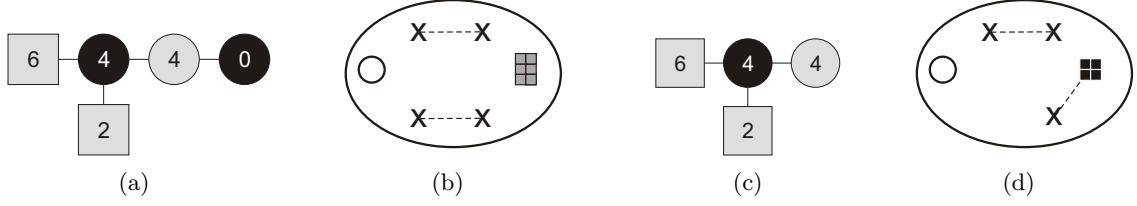


Figure 10: Superconformal tail and corresponding Riemann surface for the D_3 SO puncture with SO(2) flavor symmetry a) and b), and for the D_3 USp puncture with SO(2) flavor symmetry c) and d).

checked in a $q(t)$ expansion for the Schur (Hall-Littlewood) limit, and thus serve as a proof of principle. Here a, b, c denote respectively SO(2), USp(2) and SO(3) fugacities.

$$\begin{aligned}
\mathcal{K} \left(\begin{array}{|c|c|c|} \hline \blacksquare & \blacksquare & \blacksquare \\ \hline \end{array} \right) &= \frac{1}{(q; q)_\infty^{3/2} (t; q)_\infty^{1/2} (t^2, t^{3/2}(b/a)^\pm, t^{3/2}(ba)^\pm, tb^{\pm 2}; q)_\infty}, \\
\mathcal{K} \left(\begin{array}{|c|c|c|} \hline \blacksquare & \blacksquare & \blacksquare \\ \hline \end{array} \right) &= \frac{(t; q)_\infty^{1/2}}{(q; q)_\infty^{3/2} (t^2, q)_\infty^2 (tc^\pm, t^2 c^\pm; q)_\infty}, \\
\mathcal{K} \left(\begin{array}{|c|c|} \hline \blacksquare & \blacksquare \\ \hline \end{array} \right) &= \frac{(t; q)_\infty^{1/2}}{(q; q)_\infty^{3/2} (t^2, t^3, t^2 a^{\pm 2}; q)_\infty}.
\end{aligned} \tag{4.11}$$

The three-punctured sphere consisting of the second puncture (which has SO(3) flavor symmetry) and two maximal punctures gives the E_7 SCFT of Minahan-Nemeschansky [33], and its index can be independently (and in agreement with the above expression) computed by using the S-duality described in [7].

Note that the tail corresponding to the last puncture (SO(2) flavor symmetry) ends on a “USp(0)” gauge group, as shown in figure 10a, which also shows the corresponding Riemann surface 10b. This happens for the class of punctures described in section 4.1, but the procedure outlined above is still applicable. We find \mathcal{K} for the USp punctures with USp(2) and SO(2) flavor symmetries to be respectively given by

$$\begin{aligned}
\mathcal{K} \left(\begin{array}{|c|c|c|} \hline \blacksquare & \blacksquare & \blacksquare \\ \hline \end{array} \right) &= \frac{1}{(q, t^2, tb^{\pm 2}, t^{3/2}b^\pm; q)_\infty}, \\
\mathcal{K} \left(\begin{array}{|c|c|} \hline \blacksquare & \blacksquare \\ \hline \end{array} \right) &= \frac{1}{(q, t^2, t^2 a^{\pm 2}; q)_\infty}.
\end{aligned} \tag{4.12}$$

Here b denotes an USp(2) and a an SO(2) fugacity. These factors were checked in the Schur and Hall-Littlewood limits by comparing the index of the tail with the one for the curve, in an expansion in q and τ respectively. The superconformal tail for the SO(2) flavor symmetry is shown in figure 10c, along with the corresponding curve 10d. The index for this linear quiver is the same as the index for the one shown in figure 10a, since the “USp(0)” gauge group does not contribute to the index. From the curve this implies that (after integrating against the SO(6) polynomials)

$$\begin{aligned}
&\frac{\mathcal{A}(q, t)}{\dim_{q, t}^{\text{SO}}((\lambda_1, \lambda_2, \lambda_2))} \mathcal{K} \left(\begin{array}{|c|c|} \hline \blacksquare & \blacksquare \\ \hline \end{array} \right) P_{M \text{ SO}}^{(\lambda_1, \lambda_2, \lambda_2)} \left(at, \frac{a}{t}, a \mid q, t \right) \mathcal{K}_{\text{USp}(\times)} P_{M \text{ USp}}^{(\lambda_1, \lambda_2)} \left(t^{1/2}, t^{3/2} \mid q, t \right) = \\
&= \mathcal{K} \left(\begin{array}{|c|c|} \hline \blacksquare & \blacksquare \\ \hline \end{array} \right) P_{M \text{ USp}}^{(\lambda_1, \lambda_2)} \left(a\sqrt{t}, \frac{a}{\sqrt{t}} \mid q, t \right),
\end{aligned} \tag{4.13}$$

where λ_1 and λ_2 are Dynkin labels. This identity is true for any Dynkin labels λ_1 and λ_2 , and so taking $\lambda_1 = \lambda_2 = 0$ the representation dependent part cancels on its own and we get a relation between the \mathcal{K} -factors,

$$\mathcal{A}(q, t) \mathcal{K} \left(\begin{array}{|c|c|} \hline \square & \square \\ \hline \square & \square \\ \hline \end{array} \right) \mathcal{K}_{\text{USp}}(\times) = \mathcal{K} \left(\begin{array}{|c|c|} \hline \blacksquare & \blacksquare \\ \hline \blacksquare & \blacksquare \\ \hline \end{array} \right) . \quad (4.14)$$

We also get a relation between the SO and USp polynomials. In general, any SO puncture labeled by a Young diagram with only two columns can similarly be related to a USp puncture labeled by the Young diagram one obtains by removing the bottom two boxes of the SO Young diagram and coloring it black, thus giving a relation between the \mathcal{K} -factors and an identity involving Macdonald polynomials.

D_2 theory. Another simple example of this relation, in D_2 , is given by the colored box-shaped SO puncture with USp(2) flavor symmetry. The \mathcal{K} -factor for this puncture is

$$\mathcal{K} \left(\begin{array}{|c|c|} \hline \square & \square \\ \hline \square & \square \\ \hline \end{array} \right) = \frac{1}{(q, t^2, ta^{\pm 2}; q)_{\infty}} , \quad (4.15)$$

which satisfies

$$\mathcal{A}(q, t) \mathcal{K} \left(\begin{array}{|c|c|} \hline \square & \square \\ \hline \square & \square \\ \hline \end{array} \right) \mathcal{K}_{\text{USp}}(\times) = \mathcal{K} \left(\begin{array}{|c|c|} \hline \blacksquare & \blacksquare \\ \hline \blacksquare & \blacksquare \\ \hline \end{array} \right) . \quad (4.16)$$

We also have

$$\frac{1}{\dim_{q,t}^{\text{SO}}((\lambda, \lambda))} P_{M\text{SO}}^{(\lambda, \lambda)} \left(at^{1/2}, \frac{a}{t^{1/2}} \mid q, t \right) P_{M\text{USp}}^{(\lambda)} \left(t^{1/2} \mid q, t \right) = P_{M\text{USp}}^{(\lambda)} (a \mid q, t) . \quad (4.17)$$

At this point we can return to the A_1 interpretation of D_2 theories and include this partially closed puncture. Namely, this partial closing of the SO(4) puncture amounts to fully closing one of the two SU(2) punctures in which it decomposes in A_1 language. The coloring is simply encoded in the choice of which SU(2) becomes fully closed. More in detail, one has for the red puncture

$$P_{M\text{SO}}^{(\lambda_1, \lambda_2)} \left(at^{1/2}, \frac{a}{t^{1/2}} \mid q, t \right) = P_{M\text{SU}}^{(\lambda_1)} \left(t^{1/2}, t^{-1/2} \mid q, t \right) P_{M\text{SU}}^{(\lambda_2)} (a, 1/a \mid q, t) , \quad (4.18)$$

and for the blue puncture

$$P_{M\text{SO}}^{(\lambda_1, \lambda_2)} \left(at^{1/2}, \frac{t^{1/2}}{a} \mid q, t \right) = P_{M\text{SU}}^{(\lambda_1)} (a, 1/a \mid q, t) P_{M\text{SU}}^{(\lambda_2)} \left(t^{1/2}, t^{-1/2} \mid q, t \right) . \quad (4.19)$$

Note that when one imposes “diagonality”, the coloring becomes as expected irrelevant. For the (color-independent) \mathcal{K} -factor one has

$$\mathcal{K} \left(\begin{array}{|c|c|} \hline \square & \square \\ \hline \square & \square \\ \hline \end{array} \right) = \mathcal{K}_{\text{SU}}(\square) \mathcal{K}_{\text{SU}}(\square) . \quad (4.20)$$

Also note that when using (4.18) (or (4.19)), rewriting the Macdonald dimension in terms of SU Macdonald dimensions using (3.43), and naturally thinking of the USp(2) polynomials in terms of SU(2) polynomials, equation (4.17) is trivial.

Acknowledgments

We are grateful to Abhijit Gadde, Shlomo Razamat and Wenbin Yan for useful discussions and comments. This work is partially supported by the NSF under Grants PHY-0969919 and PHY-0969739. Any opinions, findings, and conclusions or recommendations expressed in this material are those of the authors and do not necessarily reflect the views of the National Science Foundation. The research of ML is partially funded by FCT - Portugal through grant SFRH/BD/70614/2010.

A. Macdonald Polynomials and Macdonald Operator

In this appendix we review the results from [34] that are relevant for our purposes.

A.1 Weyl invariant polynomials and the Macdonald operator

Let us start by summarizing some notational conventions, for which we follow [34]. Consider a Lie algebra \mathfrak{g} . We denote the root system of \mathfrak{g} by R and the system of positive roots by R^+ . For every root α , we denote the coroot as $\alpha^\vee \equiv 2\alpha / \langle \alpha, \alpha \rangle$. The root lattice, spanned by the simple roots $\{\alpha_i \mid 1 \leq i \leq \text{rank } \mathfrak{g} = n\}$ is denoted by Q , and its positive part by Q^+ . Finally, the weight lattice is denoted by $P = \{\lambda \in \mathbb{R}^n \mid \langle \lambda, \alpha^\vee \rangle \in \mathbb{Z}\}$, and by P^+ we denote the dominant weights, *i.e.* $P^+ = \{\lambda \in P \mid \forall \alpha \in R^+ : \langle \lambda, \alpha^\vee \rangle \in \mathbb{N}\}$. A basis for P^+ is given by the fundamental weights ω_i . The components of an arbitrary weight λ in this basis will be denoted λ_i , *i.e.* $\lambda = \sum_i \lambda_i \omega_i$. The λ_i are called the Dynkin labels of the representation. Another basis is given by the standard orthonormal basis, denoted by ϵ_i . The components in this basis will be denoted ℓ_i . On the weight lattice we can introduce a partial order as $\lambda \geq \mu \Leftrightarrow \lambda - \mu \in Q^+$.

The Weyl group W is a finite group generated by the simple Weyl reflections σ_α , for all roots α . These are defined on any weight in P as

$$\sigma_\alpha(\lambda) = \lambda - \langle \lambda, \alpha^\vee \rangle \alpha. \quad (\text{A.1})$$

The group algebra of the weight lattice P is denoted by A . It is generated by the formal exponentials e^λ , satisfying $e^\lambda e^\mu = e^{\lambda+\mu}$ and $(e^\lambda)^{-1} = e^{-\lambda}$. We can formally identify the variables x_i as $x_i = e^{\epsilon_i}$. The action of the Weyl group on P is uplifted to A as $w(e^\lambda) = e^{w\lambda}$, where $w \in W$. The subalgebra of A invariant under W is denoted by A^W , and is most easily spanned by the symmetric orbit-sums $\{m_\lambda \mid \lambda \in P^+\}$. These are defined as $m_\lambda = \sum_{\mu \in W(\lambda)} e^\mu$, where $W(\lambda)$ denotes the Weyl-orbit of λ . Another well-known basis for A^W is given by the group characters χ_λ which are given by the Weyl character formula:

$$\chi_\lambda = \frac{\sum_{w \in W} \epsilon(w) e^{w(\lambda+\rho)}}{\sum_{w \in W} \epsilon(w) e^{w\rho}}, \quad (\text{A.2})$$

where $\rho = \frac{1}{2} \sum_{\alpha \in R^+} \alpha$ is the Weyl vector and $\epsilon(w)$ is the signature of $w \in W$. The signature is defined as $\epsilon(w) = (-1)^{l(w)}$ where $l(w)$ is the minimum number of simple Weyl reflections in which w can be decomposed.

An alternative characterization of the Weyl characters is as the unique polynomials satisfying two conditions, namely that they can be written in terms of the orbit-sums for some coefficients $K_{\lambda\mu}$ as

$$\chi_\lambda = m_\lambda + \sum_{\mu \in P^+, \mu < \lambda} K_{\lambda\mu} m_\mu, \quad (\text{A.3})$$

which constrains the leading behavior, and that they are orthogonal under the Haar measure¹¹. It is these two criteria which are generalized to define the Hall-Littlewood and Macdonald polynomials for arbitrary root systems.

Let us start by introducing a 2-parameter generalization of the Haar measure

$$\Delta_M(q, t) = \prod_{\alpha \in R} \frac{(e^\alpha; q)_\infty}{(te^\alpha; q)_\infty}, \quad (\text{A.4})$$

where we used the q-Pochhammer symbols $(a; q)_\infty = \prod_{j=0}^\infty (1 - aq^j)$. We will call this measure the Macdonald measure. For $t = q$ it reduces to the Haar measure,

$$\Delta = \prod_{\alpha \in R} (1 - e^\alpha), \quad (\text{A.5})$$

and for $q \rightarrow 0$ it results in the Hall-Littlewood measure

$$\Delta_{HL}(t) = \prod_{\alpha \in R} \frac{1 - e^\alpha}{1 - te^\alpha}. \quad (\text{A.6})$$

The definition of the scalar product of two functions $f = \sum_{\lambda \in P} f_\lambda e^\lambda$ and $g = \sum_{\lambda \in P} g_\lambda e^\lambda$ is most easily written down if we first write them in terms of the x -variables introduced above. To do so we write $\lambda = \sum_i \ell_i \epsilon_i$ in the orthogonal basis, and thus $e^\lambda = \prod_i x_i^{\ell_i}$. We also introduce $\bar{g} = \sum_{\lambda \in P} g_\lambda e^{-\lambda} = \sum_{\lambda \in P} g_\lambda \prod_i x_i^{-\ell_i}$, and the shorthand notation $\oint[dx] \equiv \oint \left(\prod_i \frac{dx_i}{2\pi i x_i} \right)$. Then the inner product is defined as

$$\langle f, g \rangle = \frac{1}{|W|} \oint[dx] f(x) \bar{g}(x) \tilde{\Delta}(x), \quad (\text{A.7})$$

where $f(x) = f(x_1, x_2, \dots)$ and so forth, $|W|$ is the order of the Weyl group and $\tilde{\Delta}$ denotes one of the measures introduced above.

The generalization we were alluding to is now as follows. There exists a unique basis for A^W of functions $\{\tilde{P}_\lambda \mid \lambda \in P^+\}$ such that

$$\tilde{P}_\lambda = m_\lambda + \sum_{\mu \in P^+, \mu < \lambda} u_{\lambda\mu} m_\mu, \quad (\text{A.8})$$

where the coefficients are rational functions of q and t , such that they are orthogonal under what we called the Macdonald measure.

¹¹See below for the general discussion of the inner product.

Note that instead of normalization, one favors a constrained leading behavior. We reserve the notation \tilde{P} for polynomials satisfying this requirement. In the main text we will use polynomials orthonormal under (A.7) with the Macdonald measure (A.4), which we denote by P .

As mentioned above already, for $q = t$ the polynomials are the Weyl characters (A.3). For $q \rightarrow 0$, one has the Hall-Littlewood polynomials, which are given explicitly by

$$\tilde{P}_\lambda^{HL} = W_\lambda(t)^{-1} \sum_{w \in W} w \left(e^\lambda \prod_{\alpha \in R^+} \frac{1 - te^{-\alpha}}{1 - e^{-\alpha}} \right), \quad (\text{A.9})$$

where

$$W_\lambda(t) = \sum_{\substack{w \in W \\ w\lambda = \lambda}} t^{l(w)}. \quad (\text{A.10})$$

For general t, q , a simple expression as above for the Hall-Littlewood polynomials or Weyl-characters is absent. However, the polynomials can be generated quite easily through a determinantal formula [29].

This formula makes use of the proposition that there exists a linear operator $D : A^W \rightarrow A^W$ such that

1. D is selfadjoint, *i.e.* $\langle Df, g \rangle = \langle f, Dg \rangle$ for all $f, g \in A^W$;
2. D is triangular relative to the basis m_λ , *i.e.* for each $\lambda \in P^+$, Dm_λ is of the form

$$Dm_\lambda = \sum_{\mu \leq \lambda} c_{\lambda\mu} m_\mu;$$

3. the eigenvalues of D are distinct, *i.e.* if $\lambda \neq \mu \in P^+$ then $c_{\lambda\lambda} \neq c_{\mu\mu}$.

It is easy to understand how the existence theorem follows from this proposition. Namely, given an operator D satisfying these three properties, one can consider for each $\lambda \in P^+$ the eigenfunction \tilde{P}_λ with eigenvalue $c_{\lambda\lambda}$. One can normalize this eigenfunction such that the coefficient of m_λ equals 1. Moreover, using the selfadjointness of D and the nondegeneracy of its eigenvalues, one can argue that $c_{\lambda\lambda} \langle \tilde{P}_\lambda, \tilde{P}_\mu \rangle = \langle D\tilde{P}_\lambda, \tilde{P}_\mu \rangle = \langle \tilde{P}_\lambda, D\tilde{P}_\mu \rangle = c_{\mu\mu} \langle \tilde{P}_\lambda, \tilde{P}_\mu \rangle$, which implies that for $\mu \neq \lambda$ one has $\langle \tilde{P}_\lambda, \tilde{P}_\mu \rangle = 0$.

The proof of the proposition is given in [34] and is simply based on the construction of an operator satisfying the above three properties. To that purpose one starts by constructing for each minuscule weight π for the dual root system R^\vee ¹² the operator D_π as

$$D_\pi = \frac{1}{|W_\pi|} \sum_{w \in W} \left(\prod_{\alpha \in R^+} \frac{1 - t^{\langle \pi, \alpha \rangle} e^{w(\alpha)}}{1 - e^{w(\alpha)}} \right) T_{w(\pi), q}, \quad (\text{A.11})$$

¹²Such a minuscule weight is characterized by the requirement that $\langle \pi, \alpha \rangle = 0$ or 1 for all $\alpha \in R^+$. Note that E_8 , F_4 , and G_2 do not have minuscule weights. They can be dealt with differently. See [34].

where $T_{x,q}$ is defined by its action on the exponentials e^λ as

$$T_{x,q}e^\lambda = q^{\langle \lambda, x \rangle} e^\lambda. \quad (\text{A.12})$$

One can prove that these operators satisfy the requirements 1. and 2. The property 3. is also satisfied except for the D -series. In order to lift the degeneracy of the eigenvalues in the D -case, one constructs an appropriate linear combination of the operators D_{π_1} and D_{π_2} , where π_1 and π_2 are the two minuscule weights of $R_D^\vee = R_D$, namely the fundamental weights corresponding to the two spinor representations, *i.e.* ω_n and ω_{n-1} . For any integer $N > \frac{1}{2}n(n-1)$, where n is the rank, one considers

$$D_{\text{SO}} = \frac{1}{2}t^{-N} \left((t^N + 1)D_{\pi_1} + (t^N - 1)D_{\pi_2} \right), \quad (\text{A.13})$$

which now also satisfies property 3.

The eigenvalues of the operators D_π can be written in general as

$$c_{\lambda\lambda}(\pi) = t^{\langle \pi, \rho \rangle} \sum_{\tau \in W(\pi)} t^{\langle \tau, \rho \rangle} q^{\langle \tau, \lambda \rangle}. \quad (\text{A.14})$$

One thus has for the eigenvalues of D_{SO} in (A.13)

$$c_\lambda^{\text{SO}} = \frac{1}{2}t^{-N} \left((t^N + 1)t^{\langle \pi_1, \rho \rangle} \sum_{\tau \in W(\pi_1)} t^{\langle \tau, \rho \rangle} q^{\langle \tau, \lambda \rangle} + (t^N - 1)t^{\langle \pi_2, \rho \rangle} \sum_{\tau \in W(\pi_2)} t^{\langle \tau, \rho \rangle} q^{\langle \tau, \lambda \rangle} \right). \quad (\text{A.15})$$

A.2 More explicit expressions for the C - and D -series

Let us write the Weyl group, the Macdonald operator and its eigenvalues a little more explicit.

A.2.1 The case $C_n = \text{USp}(2n)$

The Weyl group of C_n is given by all possible permutations and sign changes of the orthogonal weights.

The dual root lattice R^\vee of C_n equals the root lattice of B_n . The unique minuscule weight of R^\vee is then the fundamental weight ω_n of B_n .

The Macdonald operator then reads explicitly [35]

$$D_{\text{USp}} \equiv D_{\pi=\omega_n^{(B_n)}} = \sum_{s_1, \dots, s_n = \pm 1} \prod_{1 \leq i < j \leq n} \frac{1 - tx_i^{s_i} x_j^{s_j}}{1 - x_i^{s_i} x_j^{s_j}} \prod_{1 \leq i \leq n} \frac{1 - tx_i^{2s_i}}{1 - x_i^{2s_i}} T_{x_i}^{\frac{s_i}{2}}, \quad (\text{A.16})$$

where T_{x_i} is defined as $(T_{x_i} f)(x_1, \dots, x_n) = f(x_1, \dots, qx_i, \dots, x_n)$.

The eigenvalues of the Macdonald operator can be written explicitly as

$$c_\lambda^{\text{USp}} \equiv c_{\lambda\lambda}(\omega_n^{(B_n)}) = \prod_{j=1}^n \left(t^{n+1-j} q^{\ell_j/2} + q^{-\ell_j/2} \right). \quad (\text{A.17})$$

A.2.2 The case $D_n = \text{SO}(2n)$

The Weyl group is given by all possible permutations and all even number of sign changes of the orthogonal weights.

The operator (A.13) reads explicitly

$$D_{\text{SO}} = \frac{1}{2} \left((D_{\pi_1} + D_{\pi_2}) + t^{-N} (D_{\pi_1} - D_{\pi_2}) \right), \quad (\text{A.18})$$

where

$$D_{\pi_1} = \sum_{\substack{s_1, \dots, s_{n-1} = \pm 1 \\ s_n = \prod_{j=1}^{n-1} s_j}} \prod_{1 \leq i < j \leq n} \frac{1 - tx_i^{s_i} x_j^{s_j}}{1 - x_i^{s_i} x_j^{s_j}} \prod_{1 \leq i \leq n} T_{x_i}^{\frac{s_i}{2}}, \quad (\text{A.19})$$

$$D_{\pi_2} = \sum_{\substack{s_1, \dots, s_{n-1} = \pm 1 \\ s_n = -\prod_{j=1}^{n-1} s_j}} \prod_{1 \leq i < j \leq n} \frac{1 - tx_i^{s_i} x_j^{s_j}}{1 - x_i^{s_i} x_j^{s_j}} \prod_{1 \leq i \leq n} T_{x_i}^{\frac{s_i}{2}}. \quad (\text{A.20})$$

Its eigenvalues can be written as

$$c_\lambda^{\text{SO}} = \frac{1}{2} \prod_{j=1}^n \left(t^{n-j} q^{\ell_j/2} + q^{-\ell_j/2} \right) + \frac{1}{2} t^{-N} \prod_{j=1}^n \left(t^{n-j} q^{\ell_j/2} - q^{-\ell_j/2} \right). \quad (\text{A.21})$$

It is important to observe here that the eigenvalues of the representation $\lambda' = \sum_{i=1}^{n-1} \ell_i \epsilon_i$ of C_{n-1} equal the eigenvalues of the representation $\lambda = \sum_{i=1}^{n-1} \ell_i \epsilon_i + 0 \epsilon_n$ of D_n . In Dynkin labels, the equivalent statement is that the eigenvalue of the representation $\lambda' = \sum_{i=1}^{n-1} \lambda_i \omega_i$ of C_{n-1} equals that of the representation $\lambda = \sum_{i=1}^{n-1} \lambda_i \omega_i + \lambda_{n-1} \omega_n$ of D_n .

B. Interwining Property of the Free Hyper Index

After some elementary algebraic manipulations and using the properties of the q -Pochhammer symbols, one can simplify the action of the conjugated Macdonald operator on the free half-hypermultiplet index for USp to

$$\begin{aligned} \hat{D}_{\text{USp}}(\mathbf{b}) \mathcal{I}(\mathbf{a}, \mathbf{b}) &\equiv \mathcal{K}_{\text{USp}}(\mathbf{b}) D_{\text{USp}}(\mathbf{b}) \mathcal{K}_{\text{USp}}^{-1}(\mathbf{b}) \mathcal{I}(\mathbf{a}, \mathbf{b}) = \sum_{\mathbf{s}_1, \dots, \mathbf{s}_{n-1} = \pm 1} \prod_{\alpha \leq \beta}^{n-1} \frac{1 - \mathbf{b}_\alpha^{-s_\alpha} \mathbf{b}_\beta^{-s_\beta} \mathbf{t}/\mathbf{q}}{1 - \mathbf{b}_\alpha^{s_\alpha} \mathbf{b}_\beta^{s_\beta}} \times \\ &\times \prod_{i=1}^n \prod_{\alpha=1}^{n-1} \frac{1}{\left(1 - \sqrt{t/q} (a_i/b_\alpha)^{s_\alpha}\right) \left(1 - \sqrt{t/q} (a_i b_\alpha)^{-s_\alpha}\right) (\sqrt{tq} a_i^\pm b_\alpha^\pm; q)_\infty}, \end{aligned} \quad (\text{B.1})$$

and for SO to

$$\begin{aligned} \hat{D}_{\pi_1}(\mathbf{a}) \mathcal{I}(\mathbf{a}, \mathbf{b}) &\equiv \mathcal{K}_{\text{SO}}(\mathbf{a}) D_{\pi_1}(\mathbf{a}) \mathcal{K}_{\text{SO}}^{-1}(\mathbf{a}) \mathcal{I}(\mathbf{a}, \mathbf{b}) = \sum_{\substack{s_1, \dots, s_{n-1} = \pm 1 \\ s_n = \prod_{i=1}^{n-1} s_i}} \prod_{i < j}^n \frac{1 - a_i^{-s_i} a_j^{-s_j} t/q}{1 - a_i^{s_i} a_j^{s_j}} \times \\ &\times \prod_{i=1}^n \prod_{\alpha=1}^{n-1} \frac{1}{\left(1 - \sqrt{t/q} (b_\alpha/a_i)^{s_i}\right) \left(1 - \sqrt{t/q} (a_i b_\alpha)^{-s_i}\right) (\sqrt{tq} a_i^\pm b_\alpha^\pm; q)_\infty}, \end{aligned} \quad (\text{B.2})$$

and

$$\begin{aligned} \hat{D}_{\pi_2}(\mathbf{a})\mathcal{I}(\mathbf{a}, \mathbf{b}) \equiv \mathcal{K}_{\text{SO}}(\mathbf{a})D_{\pi_2}\mathcal{K}_{\text{SO}}^{-1}(\mathbf{a})\mathcal{I}(\mathbf{a}, \mathbf{b}) = & \sum_{\substack{s_1, \dots, s_{n-1}=\pm 1 \\ s_n = -\prod_{i=1}^{n-1} s_i}} \prod_{i < j}^n \frac{1 - a_i^{-s_i} a_j^{-s_j} t/q}{1 - a_i^{s_i} a_j^{s_j}} \times \\ & \times \prod_{i=1}^n \prod_{\alpha=1}^{n-1} \frac{1}{\left(1 - \sqrt{t/q} (b_\alpha/a_i)^{s_i}\right) \left(1 - \sqrt{t/q} (a_i b_\alpha)^{-s_i}\right) (\sqrt{t/q} a_i^\pm b_\alpha^\pm; q)_\infty}. \end{aligned} \quad (\text{B.3})$$

Note that one can obtain (B.3) from (B.2) by inverting a_n . First, we claim that

$$\hat{D}_{\pi_1}(\mathbf{a})\mathcal{I}(\mathbf{a}, \mathbf{b}) = \hat{D}_{\pi_2}(\mathbf{a})\mathcal{I}(\mathbf{a}, \mathbf{b}). \quad (\text{B.4})$$

Second, we claim that the hypermultiplet index $\mathcal{I}(\mathbf{a}, \mathbf{b})$ intertwines the action of the SO and USp conjugated Macdonald operators,

$$\hat{D}_{\pi_1}(\mathbf{a})\mathcal{I}(\mathbf{a}, \mathbf{b}) = \hat{D}_{\text{USp}}(\mathbf{b})\mathcal{I}(\mathbf{a}, \mathbf{b}). \quad (\text{B.5})$$

While (B.4) and (B.5) are algebraic identities, checking them is highly tedious. For D_2 and D_3 , the different equalities were checked exactly. For higher ranks numerical evidence was obtained, up to rank 15, by assigning random numbers smaller than one for t and q , and random points on the unit circle for the fugacities. It would be nice to find an analytic proof. We also expect (but have not checked) that these identities admit the natural generalization to generic values of the three superconformal fugacities, with Macdonald operators replaced by elliptic RS operators.

References

- [1] D. Gaiotto, *N=2 dualities*, *JHEP* **1208** (2012) 034, [[arXiv:0904.2715](#)].
- [2] D. Gaiotto, G. W. Moore, and A. Neitzke, *Wall-crossing, Hitchin Systems, and the WKB Approximation*, *ArXiv e-prints* (July, 2009) [[arXiv:0907.3987](#)].
- [3] L. F. Alday, D. Gaiotto, and Y. Tachikawa, *Liouville Correlation Functions from Four-Dimensional Gauge Theories*, *Letters in Mathematical Physics* **91** (Feb., 2010) 167–197, [[arXiv:0906.3219](#)].
- [4] A. Gadde, E. Pomoni, L. Rastelli, and S. S. Razamat, *S-duality and 2d Topological QFT*, *JHEP* **1003** (2010) 032, [[arXiv:0910.2225](#)].
- [5] J. Kinney, J. M. Maldacena, S. Minwalla, and S. Raju, *An Index for 4 dimensional super conformal theories*, *Commun.Math.Phys.* **275** (2007) 209–254, [[hep-th/0510251](#)].
- [6] C. Römelberger, *Counting chiral primaries in N=1, d=4 superconformal field theories*, *Nuclear Physics B* **747** (July, 2006) 329–353, [[hep-th/0510060](#)].
- [7] Y. Tachikawa, *Six-dimensional D(N) theory and four-dimensional SO-USp quivers*, *JHEP* **0907** (2009) 067, [[arXiv:0905.4074](#)].
- [8] Y. Tachikawa, *N=2 S-duality via Outer-automorphism Twists*, *J.Phys.* **A44** (2011) 182001, [[arXiv:1009.0339](#)].

- [9] O. Chacaltana and J. Distler, *Tinkertoys for Gaiotto duality*, *Journal of High Energy Physics* **11** (Nov., 2010) 99, [[arXiv:1008.5203](#)].
- [10] O. Chacaltana and J. Distler, *Tinkertoys for the D_N series*, *ArXiv e-prints* (June, 2011) [[arXiv:1106.5410](#)].
- [11] O. Chacaltana, J. Distler, and Y. Tachikawa, *Nilpotent orbits and codimension-two defects of $6d$ $N=(2,0)$ theories*, *ArXiv e-prints* (Mar., 2012) [[arXiv:1203.2930](#)].
- [12] A. Gadde, L. Rastelli, S. S. Razamat, and W. Yan, *The superconformal index of the E_6 SCFT*, *Journal of High Energy Physics* **8** (Aug., 2010) 107, [[arXiv:1003.4244](#)].
- [13] A. Gadde, L. Rastelli, S. S. Razamat, and W. Yan, *Four Dimensional Superconformal Index from q -Deformed Two Dimensional Yang-Mills Theory*, *Physical Review Letters* **106** (June, 2011) 241602, [[arXiv:1104.3850](#)].
- [14] A. Gadde, L. Rastelli, S. S. Razamat, and W. Yan, *Gauge Theories and Macdonald Polynomials*, *ArXiv e-prints* (Oct., 2011) [[arXiv:1110.3740](#)].
- [15] D. Gaiotto, L. Rastelli, and S. S. Razamat, *Bootstrapping the superconformal index with surface defects*, *ArXiv e-prints* (July, 2012) [[arXiv:1207.3577](#)].
- [16] D. Gang, E. Koh, and K. Lee, *Line Operator Index on $S^1 \times S^3$* , *Journal of High Energy Physics* **5** (May, 2012) 7, [[arXiv:1201.5539](#)].
- [17] D. Gang, E. Koh, and K. Lee, *Superconformal index with duality domain wall*, *Journal of High Energy Physics* **10** (Oct., 2012) 187, [[arXiv:1205.0069](#)].
- [18] M. Aganagic, H. Ooguri, N. Saulina, and C. Vafa, *Black holes, q -deformed 2d Yang Mills, and non-perturbative topological strings*, *Nuclear Physics B* **715** (May, 2005) 304–348, [[hep-th/0411280](#)].
- [19] T. Kawano and N. Matsumiya, *5D SYM on 3D sphere and 2D YM*, *Physics Letters B* **716** (Oct., 2012) 450–453, [[arXiv:1206.5966](#)].
- [20] Y. Fukuda, T. Kawano, and N. Matsumiya, *5D SYM and 2D q -Deformed YM*, *ArXiv e-prints* (Oct., 2012) [[arXiv:1210.2855](#)].
- [21] M. Aganagic and S. Shakirov, *Knot Homology from Refined Chern-Simons Theory*, *ArXiv e-prints* (May, 2011) [[arXiv:1105.5117](#)].
- [22] M. Aganagic and S. Shakirov, *Refined Chern-Simons Theory and Topological String*, *ArXiv e-prints* (Oct., 2012) [[arXiv:1210.2733](#)].
- [23] N. Mekareeya, J. Song, and Y. Tachikawa, *2d TQFT structure of the superconformal indices with outer-automorphism twists*, *ArXiv e-prints* (Dec., 2012) [[arXiv:1212.0545](#)].
- [24] B. I. Zwiebel, *Charging the superconformal index*, *Journal of High Energy Physics* **1** (Jan., 2012) 116, [[arXiv:1111.1773](#)].
- [25] Y. Tachikawa, *On S -duality of 5d super Yang-Mills on S^1* , *Journal of High Energy Physics* **11** (Nov., 2011) 123, [[arXiv:1110.0531](#)].
- [26] E. Witten, *An $SU(2)$ anomaly*, *Physics Letters B* **117** (Nov., 1982) 324–328.
- [27] T. Nishinaka, *The gravity duals of SO/USp superconformal quivers*, *JHEP* **1207** (2012) 080, [[arXiv:1202.6613](#)].

- [28] R. Feger and T. W. Kephart, *LieART – A Mathematica Application for Lie Algebras and Representation Theory*, *ArXiv e-prints* (June, 2012) [[arXiv:1206.6379](#)].
- [29] J. F. van Diejen, L. Lapointe, and J. Morse, *Determinantal Construction of Orthogonal Polynomials Associated with Root Systems*, *ArXiv Mathematics e-prints* (Mar., 2003) [[math/0303263](#)].
- [30] M. Aganagic and K. Schaeffer, *Orientifolds and the Refined Topological String*, *JHEP* **1209** (2012) 084, [[arXiv:1202.4456](#)].
- [31] D. Gaiotto and S. S. Razamat, *Exceptional Indices*, *JHEP* **1205** (2012) 145, [[arXiv:1203.5517](#)].
- [32] P. C. Argyres and J. R. Wittig, *Infinite coupling duals of $N = 2$ gauge theories and new rank 1 superconformal field theories*, *Journal of High Energy Physics* **1** (Jan., 2008) 74, [[arXiv:0712.2028](#)].
- [33] J. A. Minahan and D. Nemeschansky, *Superconformal fixed points with $E(n)$ global symmetry*, *Nucl.Phys.* **B489** (1997) 24–46, [[hep-th/9610076](#)].
- [34] I. Macdonald, *Symmetric Functions and Orthogonal Polynomials*, *University Lecture Series 12*. American Mathematical Society, Providence, RI, 1998.
- [35] K. Mimachi, *Eigenfunctions of Macdonald’s q -difference operator for the root system of type C_n* , [q-alg/9712054](#).